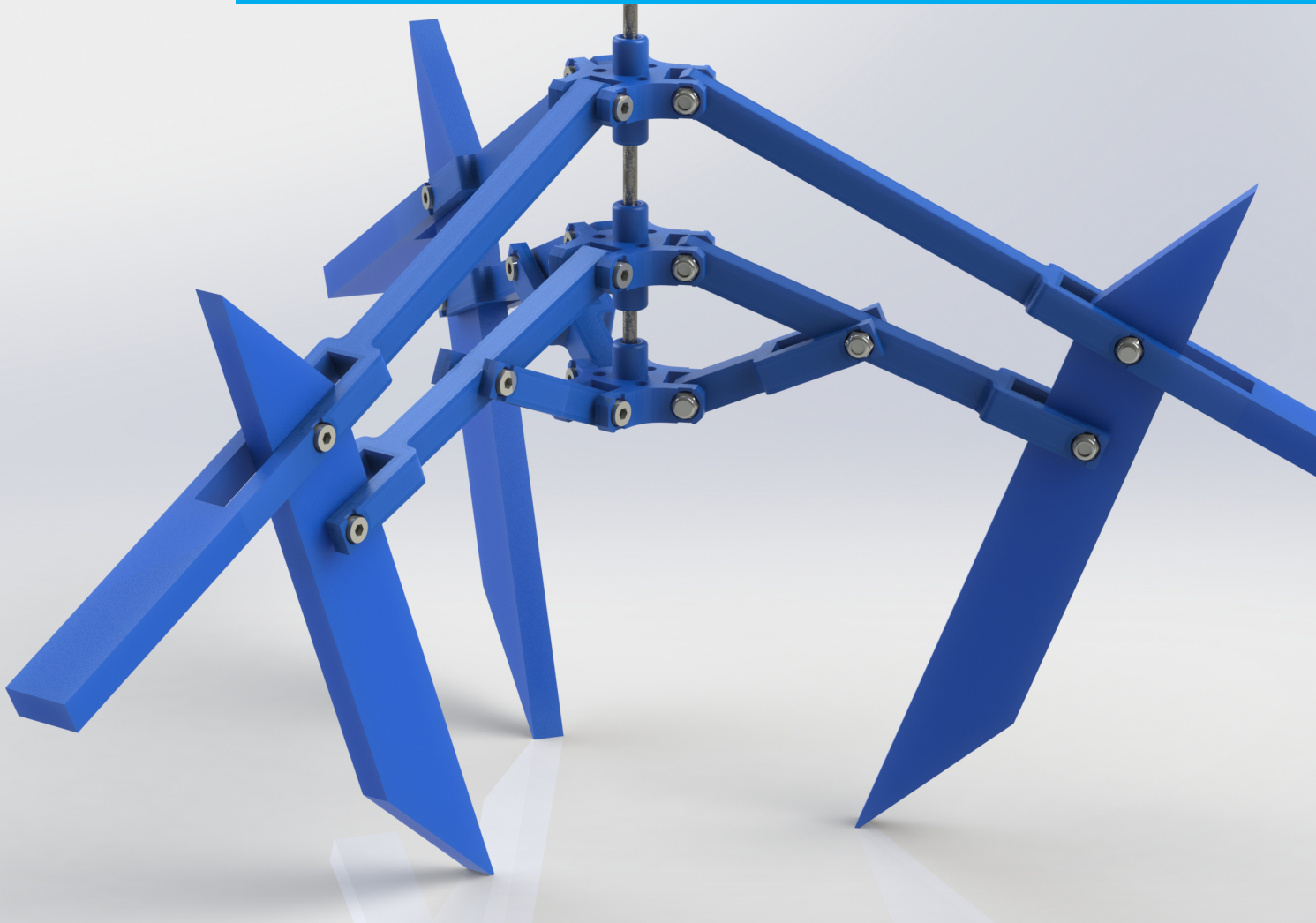


Department of Precision and Microsystems Engineering

Design of a fully actuated dynamically balanced 2-DoF gripper

H.T. Hofland

Report no : 2024.079
Coach : Prof. dr. Ir. J. L. Herder
Professor : Prof. dr. Ir. J. L. Herder
Specialisation : Mechatronic System Design (MSD)
Type of report : MSc Thesis
Date : 27-9-2024



Design of a fully actuated dynamically balanced 2-DoF gripper

H.T. Hofland (4446070)

September 4, 2024

INTRODUCTION

Due to the ever increasing need for automatisation there are many different types of grippers to pick and place objects of various shapes and sizes. These different grippers have been classified in multiple studies e.g. [1], [2], [3]. For this paper the most important distinction is made between mechanical and non mechanical grippers. Here mechanical grippers are considered to be made up from actuated elements that grasp the to be picked object by either frictional force or by geometric locking. The most common example of a mechanical gripper is the 2 fingered gripper with a friction based grip [4]. These are often available as off-the-shelf products where the right size finger and actuation range can be selected. On the other hand non mechanical grippers can make use of a variety of different ways to keep hold of their target object. They can use vacuum, adhesion, magnetism or bellows for instance. However, because the principles of balancing only apply to mechanical structures there will not be expanded on non-mechanical grippers any further.

Within the realm of mechanical grippers further division can be made by categorizing on gripper characteristics. First the amount of fingers a gripper uses to grasp the object can vary from 1,2 or 3 to full dexterous hands. Secondly the use of either rigid or soft elements is an important factor. Where a rigid element can usually apply more force, a soft element can conform to the object to secure it in place [5]. A third category can be based upon the way the object is held. This can be done with either friction or by geometrically constraining the degrees of freedom (DoF) of the object. The latter often leads to lower contact forces as these are used to hold the object directly instead of being converted to their friction counterpart [6]. A last distinction was made based on the amount of actuators used compared to the number of DoF which the gripper mechanism has. In case of a fully actuated gripper every degree of freedom has their own actuator hence the motion of the mechanism can be completely described from the actuator input. In the case of an

underactuated gripper there is a smaller amount of actuators present than the mechanism has degrees of freedom. These grippers can generally change shape based on the contact forces with the target object hence conforming to the surface of the object which can also be used to lower contact forces [7], [8], [9]. Creating an underactuation can give a simple friction based gripper much more dexterity and with that make it useful in a wider variety of gripping cases [10], [11].

When mechanisms move they generally create reaction forces on their base. These forces are caused by the changing center of mass position of the mechanism. As stated in Newtons second law $F = ma$ [12] to accelerate the mass of an object relative to another object, a force is needed. Hence changing the center of mass of a mechanism relative to its base will generate a force between the two. Balancing a mechanism then is the act of creating or altering the mechanism in such a way that the center of mass does not change relative to the base. This in turn makes that there is no force between the base and the mechanism when the mechanism moves. There are two different stages of balance which can be applied to a mechanism. The first is when the mechanism is only balanced for reaction forces. This is called shaking force balance. In this case the rotational motion of the mechanism parts can still generate moments on the base. The second stage is called full or dynamical balance. Here the reaction moments are balanced as well as the reaction forces. Shaking force balance is a prerequisite for fully balanced systems. The advantage of a balanced system over an unbalanced mechanism is that the mechanisms motion is decoupled from the motion of the base. This means that the mechanism will not move through its own motion when the base is moving the mechanism and that in turn the base does not feel the movement when the mechanism is moved. Incidentally this also means the mechanism does not need a stable base to perform its motion and that it can still perfectly function for instance on the end of a piece of string. A useful use case of a balanced gripper to exploit

this could be pick and place operations done by drones. Because balancing a pre-existing mechanism can usually only be done by adding rotating counter balance mass, balanced mechanisms are more often than not heavier than their non balanced counterparts. This means stronger joints and actuators are needed. However the control technology needed is much simpler as feed forward control is already sufficient. As a dynamically balanced system is balanced statically as well it will also carry over the characteristics that come with statically balanced mechanisms, namely that due to the balancing the mechanism does not want to move on its own as it does not have a preferred position to minimise its energy potential. Hence there are no holding forces required to keep the mechanism in place which are usually provided by feedback control. Using an inherently balanced mechanisms to build a structure can give a balanced system which does not rely on counter masses and does therefore not have the weight disadvantage of a mechanism that has been balanced after its function design was done.

Looking at these advantages and keeping in mind the use cases of high speed pick and place operations a gap seems to be present where balanced grippers can be used. However, in literature only a single example of a balanced gripper was found [13]. Moreover, this mechanism was not experimentally verified and actuated, but generated from a theoretical synthesis method and built as a proof of concept.

Because multiple design strategies and specific uses can be thought of to synthesise gripper mechanisms this paper focusses on finding a generic method to come up with these grippers. A single design is made without a predetermined use case to verify the method. This paper then presents the design and testing of a new partially inherently shaking force and shaking moment balanced 2 degree of freedom gripper. With simulations and experiments the gripper is shown to be balanced by reducing the necessary actuation forces at equal actuation speed and stroke length. Due to the higher order of freedom the gripper is able to pick and place a large range of objects with predetermined sizes. The paper starts by explaining the design methodology chosen to create the mechanism after which the resulting gripper and its characteristics are described. Next the simulations are explained which were used to verify the design is a balanced mechanism. Then the real world test setup and experiment are explained. Lastly the results of the simulations and the real world tests are shown and discussed before giving the final verdict on the

balance of the mechanism and the design method chosen.

METHOD

Design of mechanism:

In order to come up with a balanced mechanism several techniques can be used. First of all the most used method is to balance a mechanism after its function has been designed. This is done by carefully adding masses in such a way that the total center of mass (CoM) of the system will be at the joint which connects the mechanism and the fixed world for every orientation of the mechanism. Because the CoM is independent of system's position through its range of motion the mechanism does not exert dynamic forces on its base [14]. However, because all this added mass does not contribute to the core function of the mechanism this often leads to heavy mechanisms which increases the internal forces in the mechanism parts and makes that joints need to be able to support much higher loads. Therefore a more optimised design can be found by creating a mechanism in which the functional elements balance each other out without the need to add mass later. This is known as inherent balance. In order to synthesise an inherently balanced mechanism tracing beams can be inserted into an open or closed kinematic chain such that they trace the CoM. This is called the method of principal vectors and was described by Otto Fisher around 1900 [15]. A specifically interesting mechanism that arises from this method is the pantograph with counter masses which can be used to balance other mechanisms as well as being balanced by itself [16].

A third way of creating balanced mechanisms is by adding known balanced mechanisms on top of each other and then offsetting the weight of the upper mechanism with a counter mass in the base mechanism which again gets the system CoM back at the fixed world joint. As there are many mechanisms for which a balanced version has been found this gives a great number of possibilities, but again resorts to adding mass at the end. However because the mechanisms which are added are already internally balanced the mass to be added is reduced which makes this an intermediate option.

All the previously named design methods are primarily concerned with the creation of a shaking force balanced system. Although this is the first requirement in order to make a system completely dynamically balanced it is not the only one. In order to cancel out all the reaction moments at the base

the rotations of all parts have to be compensated as well. This can be done by making the previously described counter masses rotate by means of gearing systems such that they compensate the inertia of their counterparts completely. However in the creation of the gripper a different route was taken. Because the gripper would have multiple mechanical fingers there was chosen for an axisymmetric design. When the position of the fingers is fully determined by the input of the actuators that drive the mechanism and is not influenced by its surroundings as is the case with underactuated grippers, then the motion can be made completely symmetric around the CoM. Therefore the moments created by one finger will be compensated by the others without the additional weight penalty of rotating counter masses.

For the final design a fully actuated gripper with 2 DoF was synthesised built up from 2 pantograph mechanisms stacked on top of each other. These pantographs are connected at the tip of the long arms by a beam which will also act as the grippers finger. The CoM of the whole system was chosen at the base of the lower mechanism as that would also give a stationary base for the object to be picked up to be held against making an extra contact point. Figure 1 shows an early cardboard prototype of the mechanism.



Figure 1: Cardboard model of gripper design

There was chosen for a 2 DoF gripper to get greater variety in the grippable objects as no specific use case was defined for the gripper. In analysing the motion of the mechanism it was seen that the small beams of the upper pantograph were interfering with the

large beams of the lower pantograph. Fortunately the small beams of the upper pantograph can be taken out without affecting the motion of the mechanism. This led to the final mechanism which can also be thought of as a pantograph with a two beam kinematic chain on the end, the kinematic chains together would be balancing out the weight of the slider while the other slider is balanced by taking it as a point mass on the pantograph beams. In balancing both pantographs the following formulas (Equation 1) were used as described in [14]. The slider was included to keep the mechanism axisymmetric ensuring moment balancing for the mechanism motions. The slider rail will at the same time act as the base to which other objects can be connected.

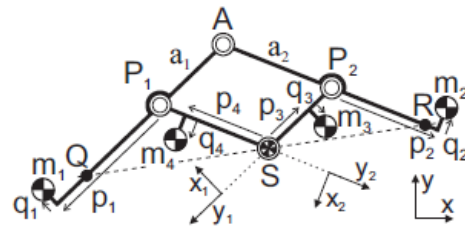


Figure 2: General 2D pantograph with masses m_1 , m_2 , m_3 , and m_4

$$\begin{aligned}
 m_1 p_1 &= m_2 a_1 + m_3 p_3 \\
 m_1 q_1 &= m_3 q_3 \\
 m_2 p_2 &= m_1 a_2 + m_4 p_4 \\
 m_2 q_2 &= m_4 q_4
 \end{aligned}
 \tag{1}$$

Design features:

Figure 3 shows the final design of the gripper. This image shows the size version of the gripper that was used during the experimental verification of the balance. As can be seen there was chosen for a 3 fingered design. This gives the minimum number of contact points needed to constrain a gripped object fully.

Because the fingers that are put in the gripper can be of any arbitrarily chosen shape as long as the weight and CoM are in the correct place for the balance, the gripper will be able to pick up a wide size range of objects. In Figure 4 the full range as derived from the SPACAR software is shown. In Figure 5 the range is confirmed with a smaller proto type. The Balls shown in the figure vary from 17 to 67 mm. For this particular prototype the mechanism would allow for objects of 10 to 88 mm, however for objects smaller than 17 mm shorter fingers need to be made

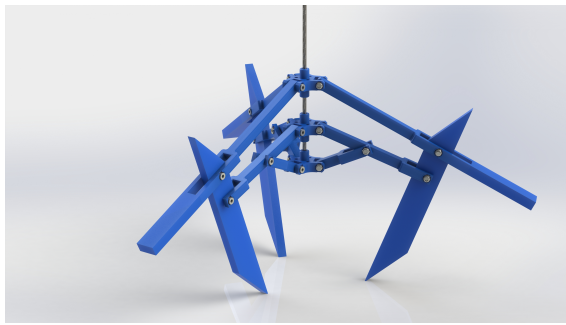


Figure 3: Final design of gripper

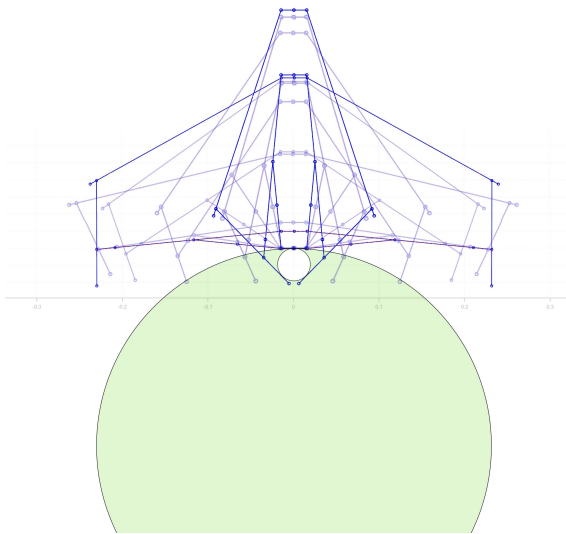


Figure 4: Range of the mechanism

to prevent self-intersection of the mechanism. The maximum size of 88 mm makes for a pinch grip where the fingers are parallel and the grip is based on friction rather than geometrical locking.

The size ratio between the long beams in the upper pantograph compared to the lower pantograph of the mechanism has in the end been chosen in such a way that the upper pantograph has a beam that is longer than the beam of the lower pantograph (see Figure 17 in Appendix B for the ratio). This ensures that even at the widest configuration of the lower pantograph a geometric lock with 60 degree angles can still be made. This geometric locking grip is preferred over a friction locked grip as the object is simply constrained in its movement instead of held by (friction) force. In the end this should lead to lower contact forces between the object and the gripper.

Simulation verification methods:

After the design of the mechanism the balance was verified with two numerical methods. First a simu-

lation was made in which the positions of the input beams was prescribed. From these the position of all the other beams was calculated by means of their joints and lengths. For the position of the CoM of the designed beams the data from the SOLIDWORKS CAD files was used for each beam individually. With the beam position and the internal CoM of all the beams the total combined CoM of all the beams was calculated. In order to account for the hardware needed to make up the joint in a physical model extra point masses were added. By looping over different input positions and combining all the mass locations with a weighted average, the change in the position of the total CoM of the system can be computed. For a balanced system this combined CoM should not move from its location as this would impose reaction forces on the base of the gripper.

Because the first simulation does not take into account any forces, moments or inertia a second simulation was made. This simulation was run by the MATLAB extension SPACAR. This is a package specifically designed to calculate motion of rigid and flexible elements. The model is setup by an array of massless beams which are interconnected via user specified joints. The beams are described as a straight line between two specified points. These points were calculated by filling in the properties of all the beams in parametric formulas which describe the joint positions. To add mass a new beam is added between the CoM of a beam, which is gathered from CAD like before, and one of the joint points of the beam of which the mass is specified in the CoM. This mass beam is then connected to the original with a fix constraint unifying the movement of the mass beam and mass point with that of the actual beam. In the end all DoF have to be determined by either an input value, an external constraint for instance a slider or the fixed world, or a joint constraint. Dependant on the type of joint indicated is which DoF are described by it. This makes that a deterministic outcome can be calculated if the given input motion does not cause a singularity or impossible configuration. When the beam structure is fully described the simulation is run based solely on the inputs and constraints. The prescribed points are only used for the initial setup. After running the simulation the forces and motions at all the separate nodes are known which can confirm both shaking force and shaking moment balance. In both simulations perfectly rigid beams and perfect joints were assumed. This is an inherent assumption in balanced mechanisms as an unknown flexibility will unbalance a system immediately.

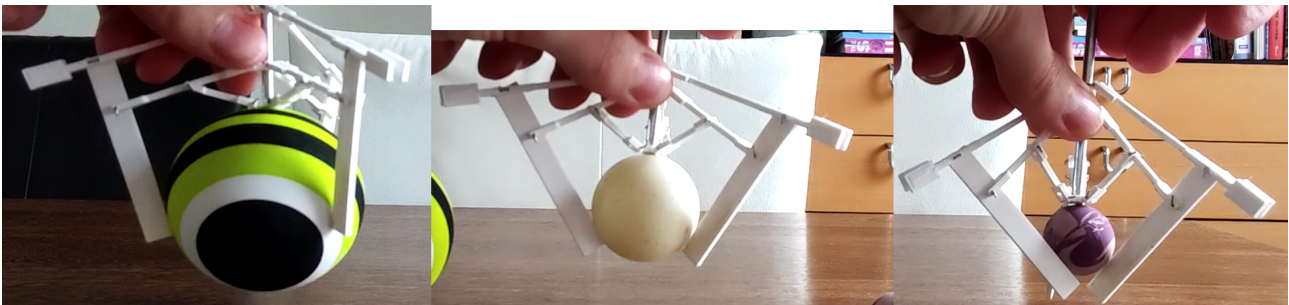


Figure 5: Real world range of the mechanism left to right 67 mm, 39 mm, 17 mm

Design of Experiment parts:

For the verification of the mechanism several different experiments can be performed. The first and easiest test is putting the mechanism in different configurations and checking if it remains in equilibrium. If this is not the case the mechanism has a lower energy state towards which it tends meaning the CoM goes down in the gravitational field. With a moving CoM the mechanism cannot be force balanced and in extension it can not be dynamically balanced. The follow up test is to agitate the mechanism by shaking it and rotating it. If this agitation leads to movement of the mechanism itself there again is a preferred state for the CoM and the mechanism is again unbalanced. When an axisymmetric design is chosen it is possible that the mechanism is moment balanced for its own motion, but when an external rotation is applied to it the mechanism has an outward tendency. This is caused by the sub mechanisms CoM. In the case of the gripper it is the CoM of one finger going outward with the rotation which is a then preferred state. Then the mechanism is not entirely dynamically decoupled from the bases' motion.

After the agitation tests have been done the mechanism will be mounted to a linear actuator. With this actuator the actuation force for a balanced version of the gripper will be compared against a non-balanced version. Because the actuator is not taken into account during the design of the gripper it is not possible to do a separate force measurement at the base of the actuator as this has to be connected to the actuator itself. Therefore forces can still travel through the actuator even if the force at the base is measured to be 0. In other mechanical balancing literature tests are done by suspending the mechanism to check if it starts moving upon actuation, however for this setup the same issue as before is encountered. Because the actuator was not taken into account there will be a change in the CoM position and therefore a force on the base of the whole system. Moreover

if the actuator was kept out of suspension while the gripper was suspended an external force will be introduced moving the suspended parts. For these reasons the actuation force measurement was chosen as a verification method for the balance.

For the actuator there was chosen to use a linear induction actuator. The working of such actuators can be explained as a normal electric stepper motor straightened out. Where the magnetic stator is now a rod moving through the electromagnetic field made by the coils in the static base of the actuator. The advantage of this type of actuator is that it can reach much higher velocities than more common spindle drive linear actuators. This makes that the force the mechanism exerts on its base in case of an unbalance will be much greater. Another common high-speed linear actuator is a pneumatic actuator, but this does not have any positional or force feedback. The reached position in this actuator will be determined by the equilibrium between the force of the mechanism or the end stop and the gas pressure on the piston.

The actuator has a positioning repeatability of $\pm 0,150$ mm and an accuracy of $\pm 0,5$ mm. With the control electronics from the supplier the current can be measured and with an online user interface the speed, stroke length and end positions can be set. As an input signal a binary 5 V signal is used where the switch from off to on indicates extension to the set length in the UI. This signal is made with an Arduino UNO which calculates the timing of the switch based on the input extension frequency (how many times per minute should the actuator go back and forth). The Arduino code can be seen in Appendix K.

In order to gain positional data a 24 step rotary encoder was attached to the mechanism with a gearing system. A gearing rack was bolted to the magnetic rod of the actuator by means of two friction based clamps. The rotary encoder was connected to the rack via a single gear. One full rotation of the encoder

leads to 42 mm (linear) travel of the gear. Hence this gave a measurement precision of ± 0.875 mm. Despite this being larger than the positional precision of the actuator no gearing reduction was introduced because this would force higher rotational speeds than the specifications of the encoder allow for.

To measure the force exerted by the actuator an amperage measurement was done between the power supply and the actuator. Combining this with the set supply voltage gives an electrical power. For the measurement a ACS712 20 A range current sensor was used. This sensor gives an analogue output voltage of 0 to 5 V for a range of -20 to +20 A. The Arduino analogue input has 10-bit range for 0 to 5 V hence a current difference of ± 0.02 A can be measured. From the position and electrical power the actuation force can be calculated assuming a lossless system.

$$F = \frac{U I \Delta t}{\Delta x} \quad (2)$$

In the end the electric circuit is build up from three parts: 1) power circuit for the actuator, 2) position measurement circuit with the rotary encoder, 3) amperage measurement circuit.

The full electric schematic can be seen in Appendix A

The test setup is shown in Figure 6

Experiment description:

Shaking test:

The first test is to hold the base of the mechanism in different orientations and see if it moves due to the influence of gravity. This would indicate a preferred position (lower energy solution) which means the CoM moves with the movement of the mechanism. When, after holding the mechanism in any orientation of the base, the mechanism does not move on its own it can be adjusted to any different mechanism position by hand while holding the base in the same orientation. Doing this for different positions for both sliders and different base orientations gives a good indication for balance behaviour. For this experiment the base will be held at a base orientation of approximately 0, 30, 45, 60, 90, and 180 ° and both sliders will be put in 3 different positions each testing at least $6 \times 9 = 54$ different orientation position combinations.

Secondly after putting the mechanism in the different orientations and positions as described above the base will be shaken. The forces transferred through the base should not affect the position of the mechanism itself. Only the position of the complete mechanism

in space should change. If the position of the mechanism parts does change due to the shaking force that means the mechanism is not force decoupled from its base which is an inherent property of shaking force balanced mechanisms.

As a last unactuated test the base will be rotated at the earlier specified base orientation angles. Because the mechanism is made axisymmetric it can be that even though it is dynamically balanced for the slider movements, the CoM of the individual fingers goes towards and away from the base. This means higher rotational velocity leads to centripetal forces on these CoM's which in turn change the position of the mechanism.

Actuated test:

For the test with the actuator five different cases will be tested. 1) actuator and measurement system separately, 2) top slider actuated while holding the bottom slider in place with a (assumed) balanced gripper configuration, 3) bottom slider actuated while holding the top slider in place with a (assumed) balanced gripper configuration, 4) top slider actuated while holding the bottom slider in place with a unbalanced gripper configuration, 5) bottom slider actuated while holding the top slider in place with a unbalanced gripper configuration. 1) will give a baseline of power usage for the actuator and measurement system which can be compared to the other cases. The other four cases test the movements of the top and bottom pantograph separately in such a way that the other pantograph cannot move and hence disturb the balance. The unbalance will be made by installing a different unbalanced finger beam in the mechanism in only 1 of the arms making the design asymmetric and the sub mechanism unbalanced. Per case at least 100 back and forth movement cycles will be made and logged in a text format data file. The data included will be: time elapsed from start of running code, position measured by rotary encoder, input from Arduino controller in binary, text version of the input (high/low for easier interpretation operator during test), Amperage measurement value in 10-bit number. This data is logged by a opensource software called CoolTerm that reads the Arduino serial monitor.

RESULTS

Simulation results:

Position simulation results

In Figure 7 the graphical representation of the positional simulation is shown. The code computes the

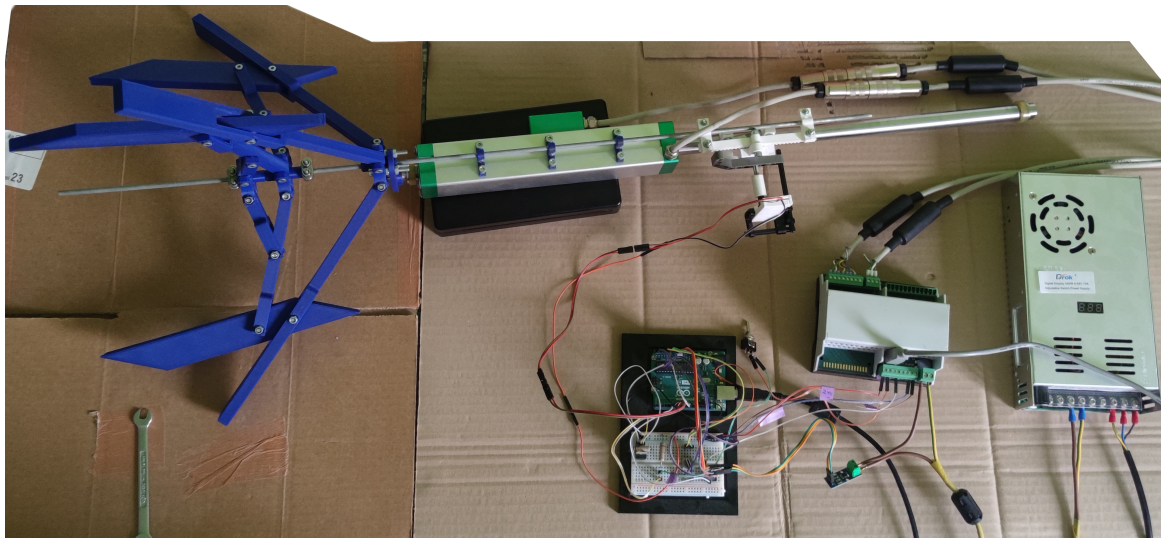


Figure 6: Actuated test setup

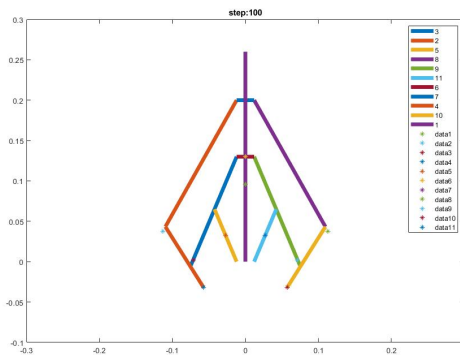
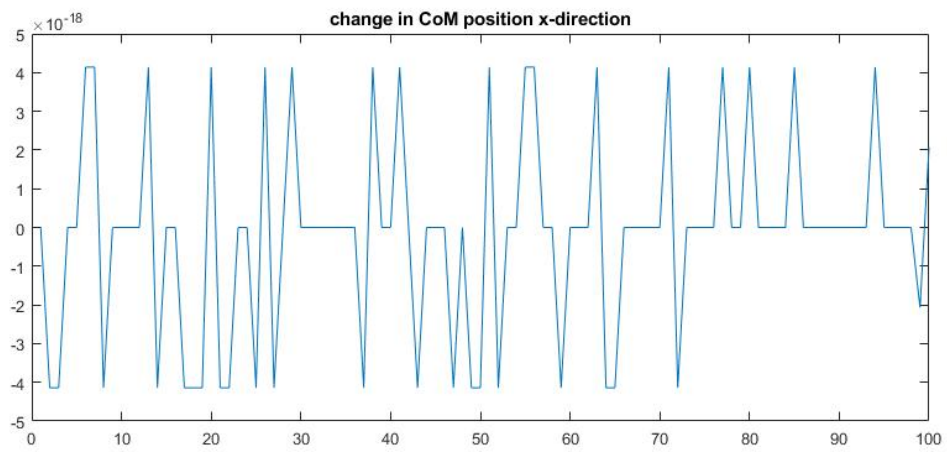


Figure 7: Position simulation graphic

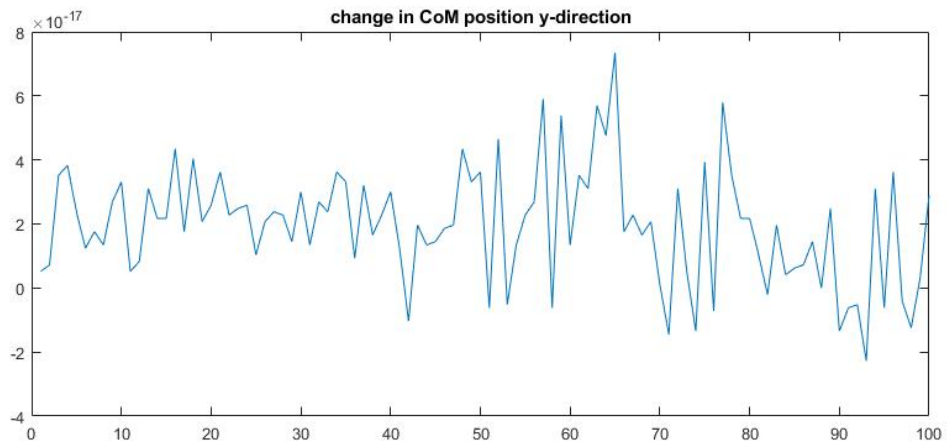
position of every beam based on the input of the two sliders. Afterwards it calculates the combined CoM of all the beam CoMs and masses. In Figure 8a and 8b the CoM positions in x and y respectively are shown. The x-axis of the plots are the step number in the simulation where the sliders are moved linearly from 10 to 170 mm for slider 1 (lower slider) and from 70 to 200 mm for slider 2 (upper slider) in 100 steps. It can be seen that for this simulation the CoM is computed to change in the order of 10^{-18} m in the x-direction and 10^{-17} m in the y-direction. These fluctuations can be explained by the numerical error of the numbers used in the calculation.

SPACAR simulation results

The SPACAR rigid body simulation results for 4 distinct cases have been calculated as can be seen in Appendix C. The cases are 1) both sliders move from roughly the middle of their range of motion away from each other, 2) the lower slider moves from top to bottom of its range while upper slider is held still 3) the upper slider moves from the bottom to the top of its range while the lower slider stays still, and 4) Both sliders move from top to bottom together. Figure 9 shows the graphical representation of the simulated movement of the first case. Here the red dotted lines are the initial position and the blue lines are the current position of the mechanism at the time selected on the slider underneath. The circles represent the nodes which are used to create the beams that make up the mechanism, represent the mass, and are used as hinge, slider, or rotational joints. In Figure 10 the change in the CoM position can be seen for case 1. Similar to the positional simulation we see numbers in the order of 10^{-17} m which is at the numerical precision limit of the numbers used in MATLAB. Figure 12 shows the corresponding reaction forces on both the sliders separate (yellow and orange), the sum of the forces on both sliders combined (purple) and the reaction force at the base (blue). Note that these forces are internal in the mechanism and in the case where the mechanism is balanced these forces should be equal and opposite (blue = -purple). This is because the mechanism will not add to the forces acting on the base and hence the external actuator forces are the same as the base forces. The reaction forces calculated at the base minus the actuation forces for



(a) CoM-x



(b) CoM-y

Figure 8: Simulated Change in CoM position

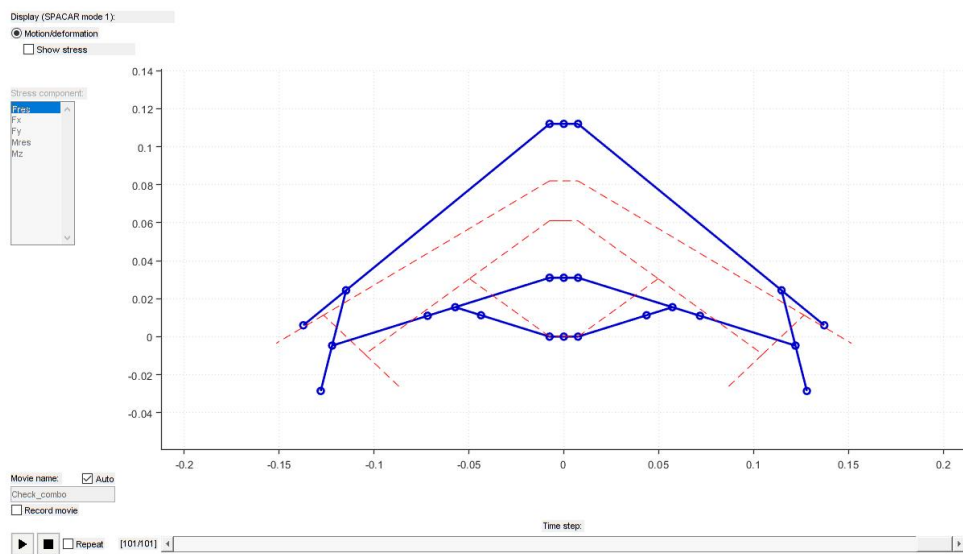


Figure 9: SPACAR simulated movement with red initial and blue current state of mechanism

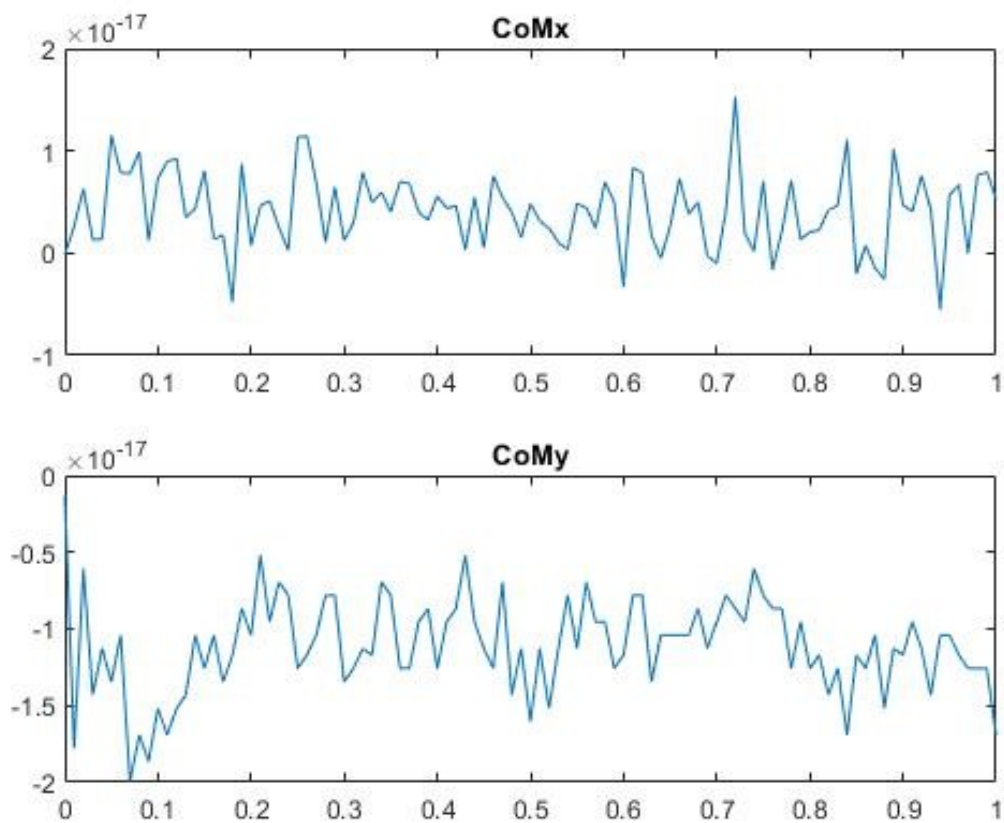


Figure 10: SPACAR simulation CoM change for case 1

case 1 can be seen in Figure 11. The same graphs for all four cases are shown in Appendix C. In all four cases it is seen that the forces are in the order 10^{-16} or 10^{-17} N, which again is the numerical precision limit for the simulation. From this it is concluded that the simulated mechanism is balanced. As the separate and the combined motions do not generate any force.

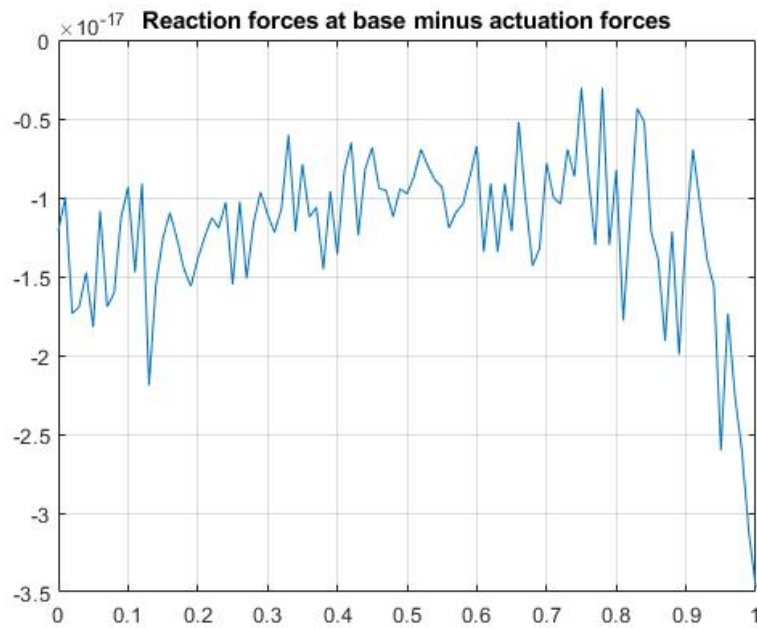


Figure 11: Case 1: reaction forces when both sliders go from middle away from each other

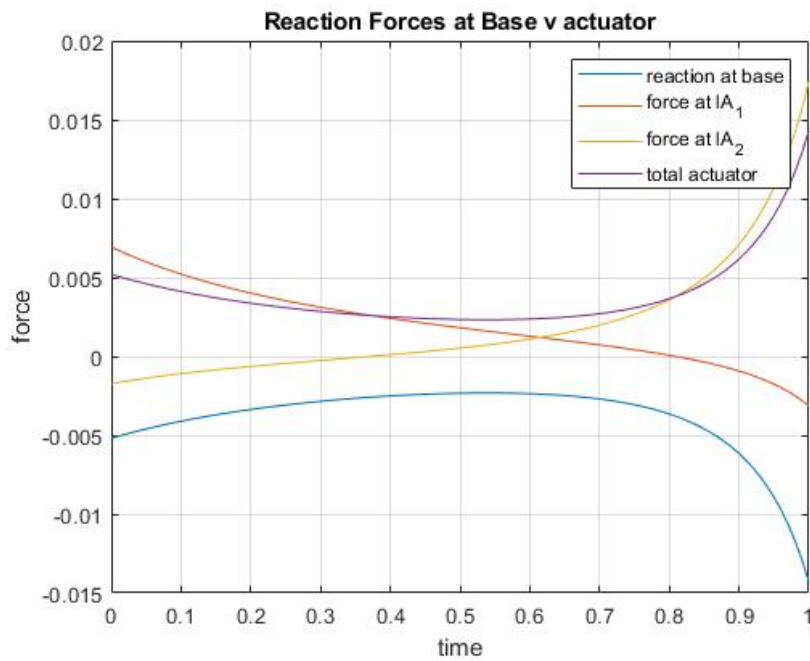


Figure 12: SPACAR simulation sum of actuation forces and base reaction forces are equal and opposite

Experimental results:



Figure 13: Different slider positions shaking test

Shaking test results

When the mechanism was assembled and suspended from the base it was seen that it did not move when being picked up or carried around. This was a good first sign because before the joint point masses were implemented in the SPACAR model the hardware immediately moved up and down the base when the base was lifted until it reached the preferred state. With this initial stability in free suspension the mechanism was put into different positions as previously described and shown in Figure 13 and in none of these positions did the mechanism show any movement or instability. Also, when shaking the base there was no internal movement seen in any of the different positions only a translation of the mechanism as a whole. All of this combined gives a good indication that the mechanism is shaking force balanced. Lastly when the mechanism was spun around the axis it was observed that there was movement. This shows that the mechanism is not decoupled from a rotation of the base. This means the mechanism seems to be balanced for the movement of the mechanism itself, but in the end is not completely dynamically balanced.

Actuated test results

Figure 14 shows the acquired mean force data from the different load cases plotted on top of each other for comparison. The graph with the complete standard deviation can be seen in Appendix D. First it

was noticed that the standard deviation (shaded area) was very large compared to the mean value where often the peaks in the standard deviation were a factor 20 larger than the mean. Looking in the raw data it was found that there was drift present in the position data during the measurement. This makes that when the position goes up more during one cycle than on other cycles it a higher actuation force is calculated. Because of the high number of cycles per load case it is assumed that this random drift noise does not influence the mean as the random drift noise cancels out when averaged. Where Figure 14 is the zoomed in version on the means Figure 19a shows the complete data including the full standard deviations for all the load cases. In Figure 14 it can be seen that the force required for the actuator and measurement system alone is a dominant factor in the force required for the total system with gripper included. In Figure 15a the mean force difference between the load case with the unbalanced upper pantograph gripper and the free actuator is shown. This was done by subtracting the mean of the actuator and measurement system alone from the mean of the unbalanced upper pantograph. The same comparative graphs for the other four test cases are shown in Appendix E. Figure 15b is a similar comparison, but now between the case of the unbalanced upper pantograph and the balanced gripper. From this we can determine the influence of the balancing on the required actuation force. The force profile between balanced and unbalanced load case compared to the free actuator is seen to be very similar for both the top and bottom slider. In both cases the peak forces are higher in the unbalanced case compared to the balanced case. This is what can be expected for balanced mechanisms as these do not push the actuator in a particular direction as their movement does not generate force on the base. In Figures 15b and 20f the comparison is made between the balanced and unbalanced versions of the same slider. Over the whole motion the reduction in force from balancing the mechanism seems about 0,5 N where the unbalanced gripper needs around 1 N and the balanced gripper 0,5 N. This is a reduction of 50%. In the peaks the difference is more in the range of 0,2 N where the peak for the top slider in the unbalanced case is 2,38 N compared to 2,17 N for the balanced case. For the bottom slider the peak is 1,26 N for the unbalanced gripper and 1,09 N for the balanced gripper. This means a force reduction of 9% for the top slider and 14% in the bottom slider.

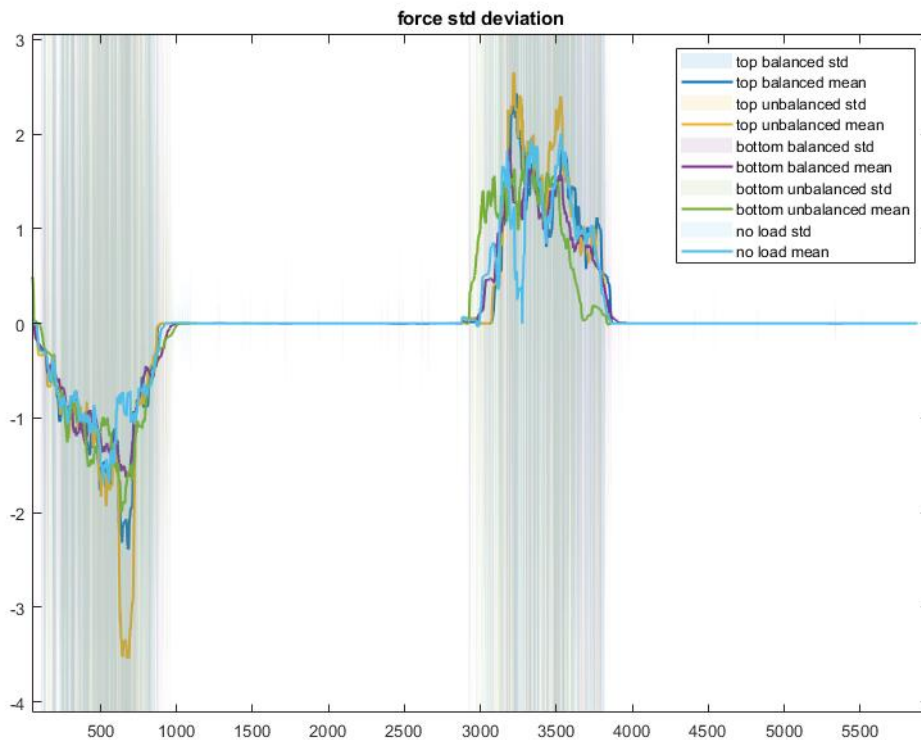


Figure 14: Measured forces actuated test 5 different load cases zoomed in on mean values

DISCUSSION

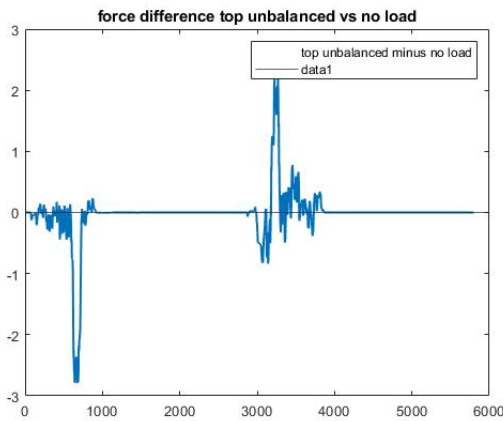
While the proposed mechanically balanced gripper shows the chosen design method works for generating balanced mechanisms and functions well as a gripper in all tests and simulations, some notes have to be made.

First of all the method of design and verification chosen did not allow for the shaking forces to be measured directly. Hence the indirect method of going by the actuation forces had to be used. This makes interpreting the data gathered from the actuated test more difficult. The shaking forces are combined with other influences such as friction in sliders and joints and possible inconsistency in the electric power used to make the actuator move masking the sought after shaking force values. As the results from the three other tests indicate the design is balanced and a reduction in the actuation forces is seen in the actuated test the balance seems to be verified. If this method will be used in future work it is critical to back up the actuated test by the simulations. Also the addition of the non-actuated test in the real world can already reveal unbalanced behaviour even if the simulations give a "balanced" result as some simple components like joints may have been overlooked in

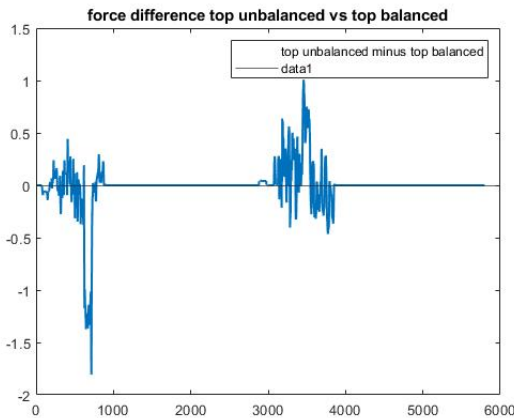
initial simulations.

For the actuated test the force required for the actuator without any additional load was very high compared to the load cases with the gripper. Therefore the actuator behaviour obscures the force differences between the different gripping scenarios. In order to solve this it would be better to make the gripper out of a more dense material to make it heavier. This will also make the difference between the balanced and unbalanced cases more visible. However due to manufacturing constraints and mechanism complexity there was chosen for 3D printed plastic which compared to most common machining metals is very light weight.

According to the manufacturer the 3D printer itself has a printing precision of $\pm 0,1$ mm. Together with tolerances of the other hardware i.e. nuts, bolts, and washers a perfect balance can never be reached unless precision measurement and subsequent piece-by-piece tailoring of the counter mass parts can be done. So while the simulations show that the intended gripper is perfectly balanced this will not be the case for the real world prototype. However as it is observed that the mechanism sliders move with very little friction and because there was an unbalance



(a) Force top slider in unbalanced gripper minus force non loaded actuator



(b) Force top slider in unbalanced gripper minus force top slider in balanced gripper

Figure 15: Mean actuation force comparison for different load cases

seen in an earlier version of the gripper it is known that the friction forces are low compared to what the unbalance forces would be if the model was not sufficiently balanced. Therefore it is assumed that the observed balance is not a result of the friction forces holding the mechanism in place.

The chosen method of adding inherent balance elements introduces additional weight to compensate for the addition, potentially negating some of the benefits of using inherently balanced elements to begin with. In order to take full advantage of the inherent balance the mass tracing beam method might be a better option, however this leads to much more complex designs and gives less freedom to design the function of a mechanism. In the end it was calculated that around 60% of the weight of the mechanism was there for balancing purposes. A more precise number can not be given as the gripper fingers are at the

same time used as a balancing beam. The rest of the purely balancing mass is located at the finger side on the upper pantograph.

As was shown in the shaking test the gripper is not fully decoupled from the rotational motion of its base. While all the internal motions will not apply a force on the base of the gripper, the base will apply some force to the gripper when in motion. For high-speed operations where the gripper is placed as an end effector on an actuating arm this might lead to the need for additional actuation force on the mechanism. In many applications however there will not be constant and or high rotational velocity, here the shaking force balance and internal shaking moment balance will still be beneficial for control purposes and vibration reduction.

Furthermore, because the actuator is not incorporated in the gripper, the system as a whole will generate a force on its base due to the shifting CoM of the actuator. This negates some of the advantages of choosing a balanced gripper design. Because the gripper itself has a stationary CoM it does not contribute to this force.

In general the method chosen as a whole seems to be a valid way of generating a mechanically balanced mechanism. As the design presented is a planar mechanism multiplied 3 fold around an axis this method will also work for any other multiplication larger than 1, most notably the subclass of (fully planar) 2D mechanisms. The lower limit on the multiplication for this mechanism is found in the axisymmetric choice of design which is not present with only a single finger. For the case of non-planar mechanisms it is assumed that adding already balanced mechanisms and balancing out the remaining forces will also work, however the mathematics for the simulations will become much more complex.

CONCLUSION

In this paper a partially balanced 2 DoF gripper was designed and verified. In two different simulations the design was shown to be completely balanced for all internal movements after which a prototype was made. In the real world actuated test it provided a 50% force reduction compared to the imbalanced version in most of the motion and around 10% force reduction in the parts where the forces peak. The gripper is shown to be able to pick up a large range of objects from about 11% up to 100% of its own width. For different applications this gripper can be scaled to desired dimensions and the finger length and shape can be adjusted to need. In the end it is concluded

that the chosen method of adding (inherently) balanced elements to create new balanced mechanisms is a valid approach.

REFERENCES

- [1] G. J. Monkman, S. Hesse, R. Steinmann, and H. Schunk, *Robot Grippers*. John Wiley & Sons, Ltd, 2006.
 - [2] K. Tai, A.-R. El-Sayed, M. Shahriari, M. Biglarbegian, and S. Mahmud, “State of the Art Robotic Grippers and Applications,” *Robotics*, vol. 5, p. 11, June 2016. Number: 2 Publisher: Multidisciplinary Digital Publishing Institute.
 - [3] Z. Samadikhoshkho, K. Zareinia, and F. Janabi-Sharifi, “A Brief Review on Robotic Grippers Classifications,” in *2019 IEEE Canadian Conference of Electrical and Computer Engineering (CCECE)*, pp. 1–4, May 2019. ISSN: 2576-7046.
 - [4] L. Birglen and T. Schlicht, “A statistical review of industrial robotic grippers,” *Robotics and Computer-Integrated Manufacturing*, vol. 49, pp. 88–97, Feb. 2018.
 - [5] M. Ceccarelli, G. Figliolini, E. Ottaviano, A. Mata, and E. Criado, “Designing a robotic gripper for harvesting horticulture products,” *Robotica*, vol. 18, Jan. 2000.
 - [6] A. Bicchi and V. Kumar, “Robotic grasping and contact: a review,” in *Proceedings 2000 ICRA. Millennium Conference. IEEE International Conference on Robotics and Automation. Symposia Proceedings (Cat. No.00CH37065)*, vol. 1, pp. 348–353 vol.1, Apr. 2000. ISSN: 1050-4729.
 - [7] T. Laliberté, L. Birglen, and C. Gosselin, “‘Underactuation in robotic grasping hands’,” *Japanese Journal of Machine Intelligence and Robotic Control*, vol. 4, pp. 77–87, Jan. 2002.
 - [8] G. Kragten, “Underactuated Robotic Hands for Grasping in Warehouses,” in *Automation in Warehouse Development*, pp. 117–131, London: Springer London, 2012.
 - [9] H. Heidari, M. J. Pouria, S. Sharifi, and M. Karami, “Design and fabrication of robotic gripper for grasping in minimizing contact force,” *Advances in Space Research*, vol. 61, pp. 1359–1370, Mar. 2018.
 - [10] R. R. Ma, A. Spiers, and A. M. Dollar, “M2 Gripper: Extending the Dexterity of a Simple, Underactuated Gripper,” in *Advances in Reconfigurable Mechanisms and Robots II* (X. Ding, X. Kong, and J. S. Dai, eds.), Mechanisms and Machine Science, (Cham), pp. 795–805, Springer International Publishing, 2016.
 - [11] P. N. Koustoumpardis, K. X. Nastos, and N. A. Aspragathos, “Underactuated 3-finger robotic gripper for grasping fabrics,” in *2014 23rd International Conference on Robotics in Alpe-Adria-Danube Region (RAAD)*, pp. 1–8, Sept. 2014.
 - [12] I. Newton, *Philosophiae naturalis principia mathematica*. Jussu Societatis Regiae ac Typis Josephi Streater. Prostat Venales apud Sam. Smith ad insignia Principis Walliae in Coemiterio D. Pauli, aliosq, nonnullos Bibliopolas, 1687.
 - [13] v. d. Wijk, Volkert, *Methodology for analysis and synthesis of inherently force and moment-balanced mechanisms*. University of Twente, 2014. OCLC: 6893348902.
 - [14] V. van der Wijk, *Methodology for analysis and synthesis of inherently force and moment-balanced mechanisms: theory and applications*. PhD, University of Twente, Enschede, The Netherlands, Apr. 2014. ISBN: 9789036536301.
 - [15] V. van der Wijk and J. L. Herder, “Synthesis method for linkages with center of mass at invariant link point — Pantograph based mechanisms,” *Mechanism and Machine Theory*, p. S0094114X11001868, Oct. 2011.
 - [16] V. H. Arakelian and M. R. Smith, “Shaking Force and Shaking Moment Balancing of Mechanisms: A Historical Review With New Examples,” *Journal of Mechanical Design*, vol. 127, pp. 334–339, Mar. 2005.
-

APPENDIX A
ELECTRICAL DIAGRAM

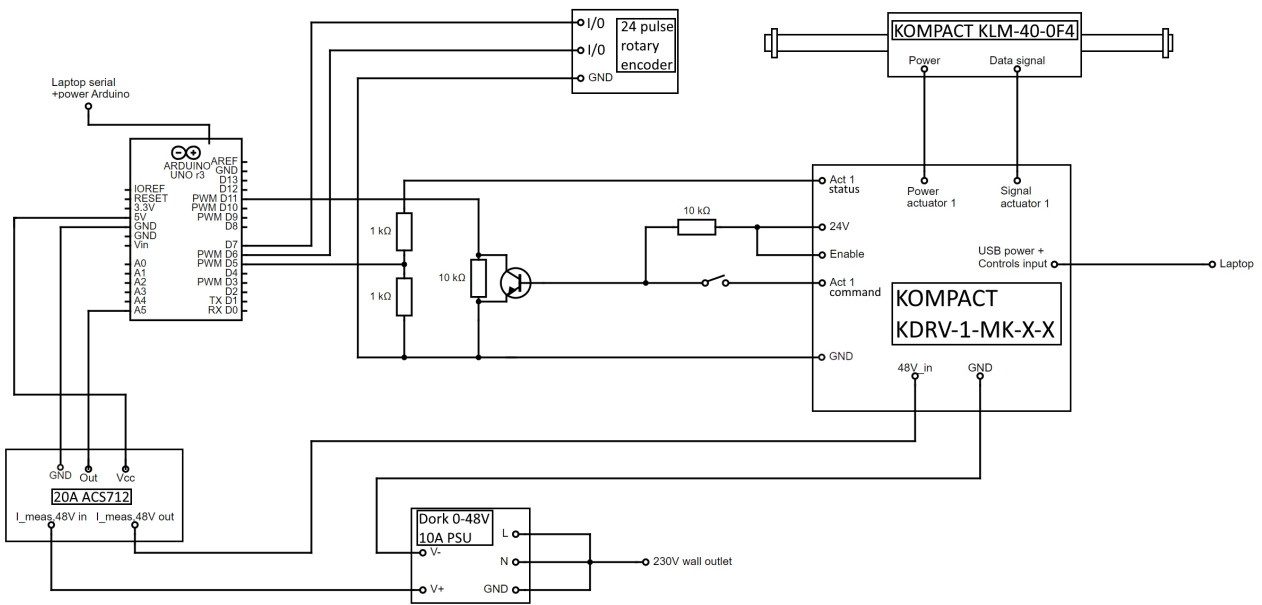


Figure 16: Setup actuated test circuit

APPENDIX B
BEAM SIZING

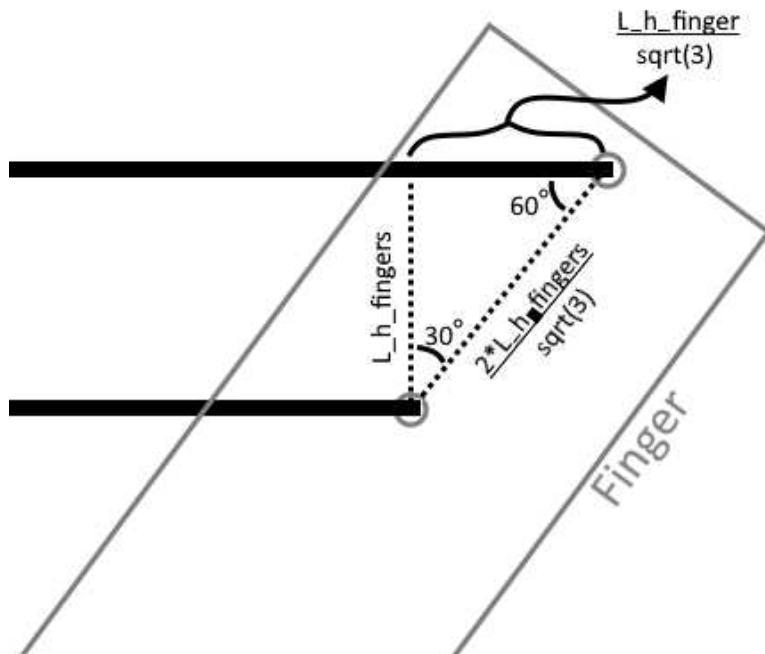
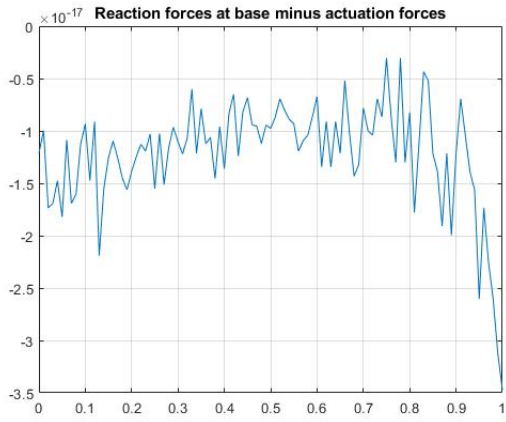
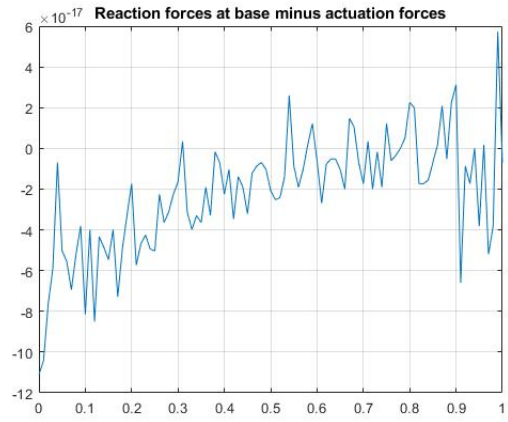


Figure 17: Ratio between finger height and length

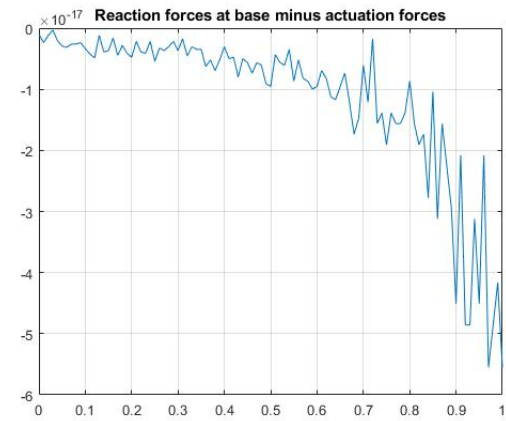
APPENDIX C
SPACAR SIMULATION ALL CASES



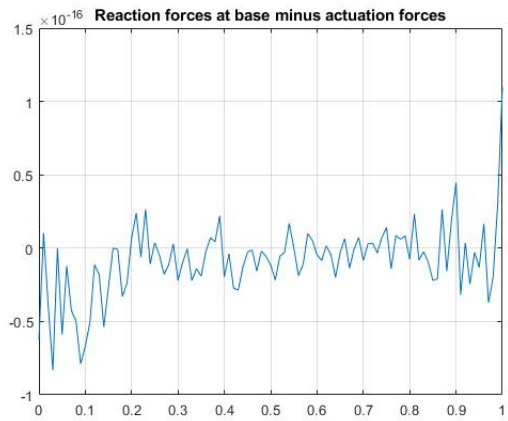
(a) Case 1: reaction forces when both sliders go from middle away from each other



(b) Case 2: reaction forces when lower slider goes from top to bottom



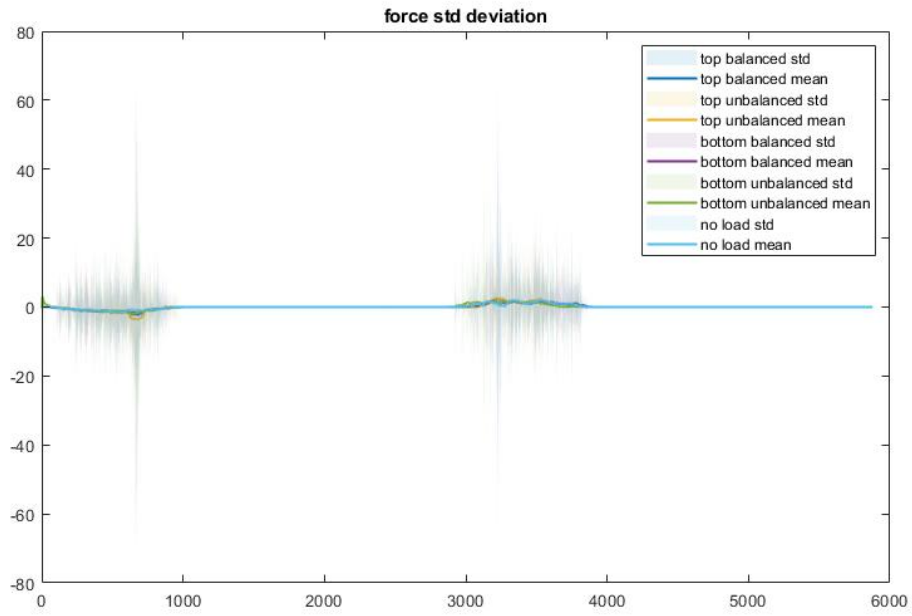
(c) Case 3: reaction forces when upper slider goes from bottom to top of range



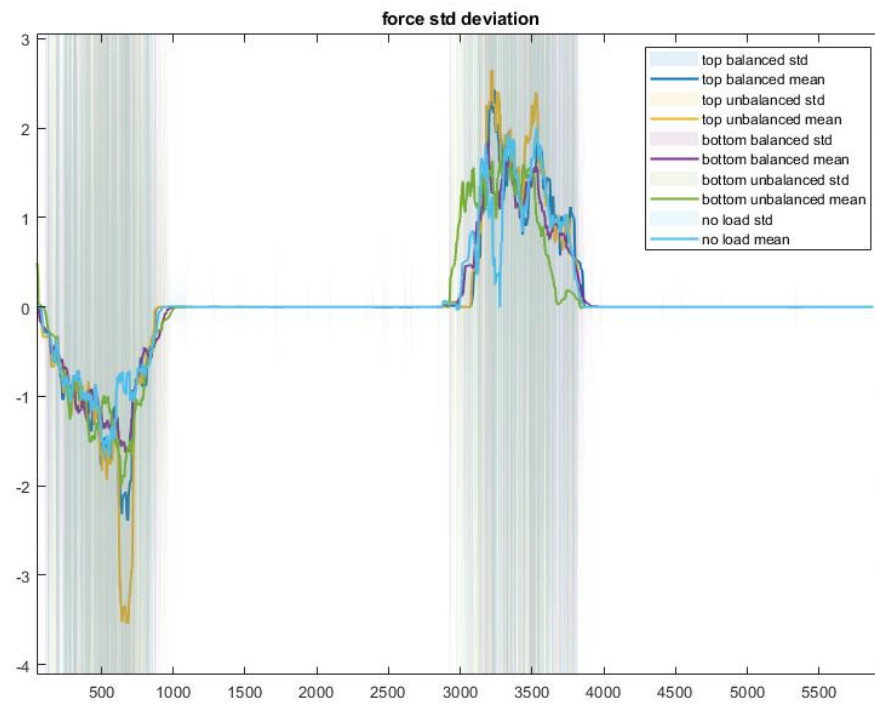
(d) Case 4: reaction forces when both sliders move from top to bottom together

Figure 18: SPACAR Reaction forces in different load cases

APPENDIX D
ACTUATED TEST ALL CASES



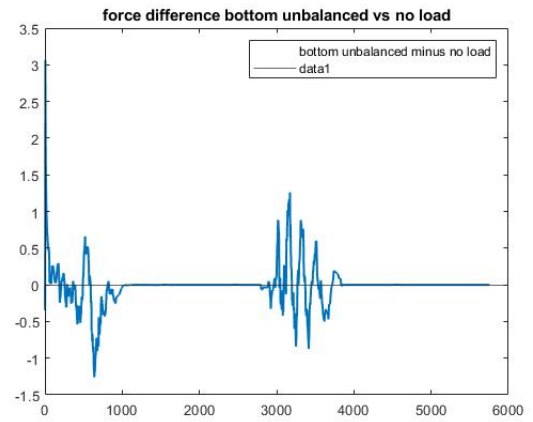
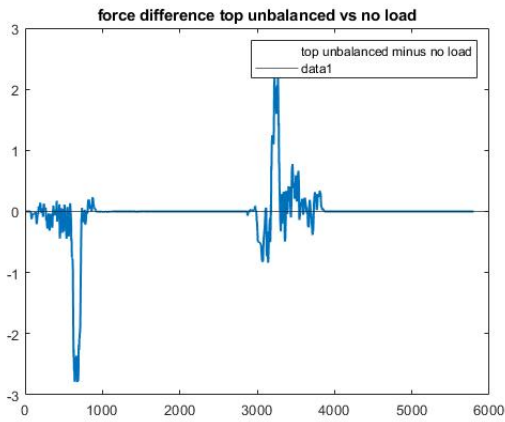
(a) Full measurements



(b) Zoomed on to mean

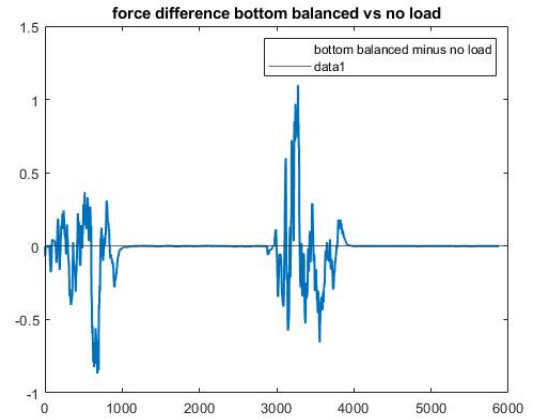
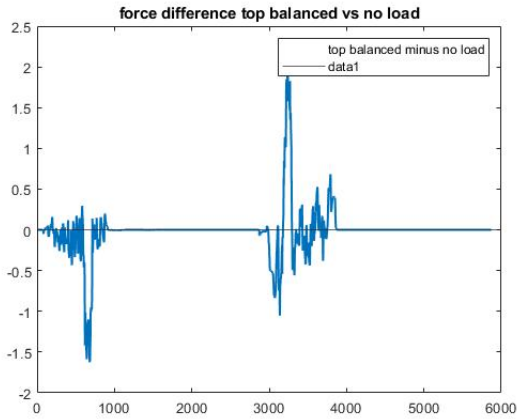
Figure 19: Measured forces actuated test 5 different load cases

APPENDIX E
ACTUATED TEST FORCE COMPARISON



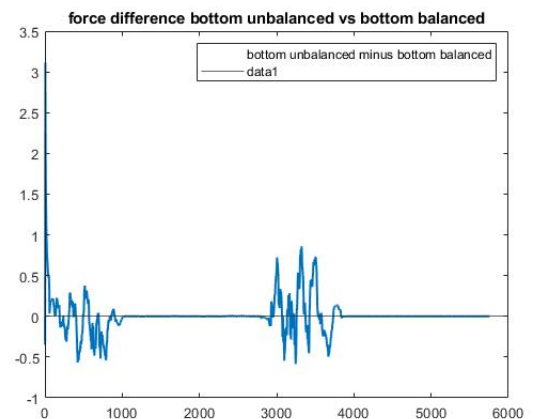
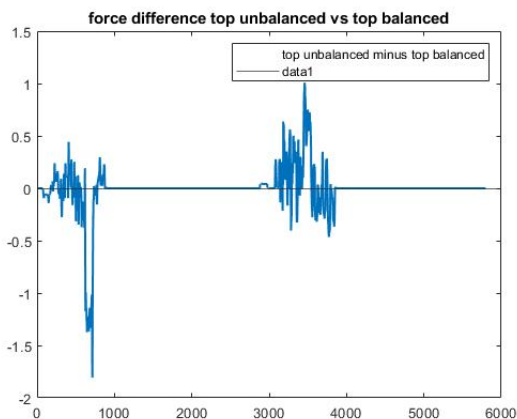
(a) Force top slider in unbalanced gripper minus force non loaded actuator

(b) Force bottom slider in unbalanced gripper minus force non loaded actuator



(c) Force top slider in balanced gripper minus force non loaded actuator

(d) Force bottom slider in balanced gripper minus force non loaded actuator

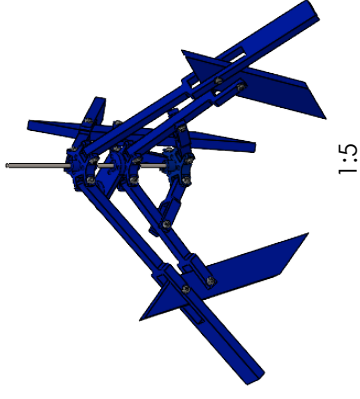
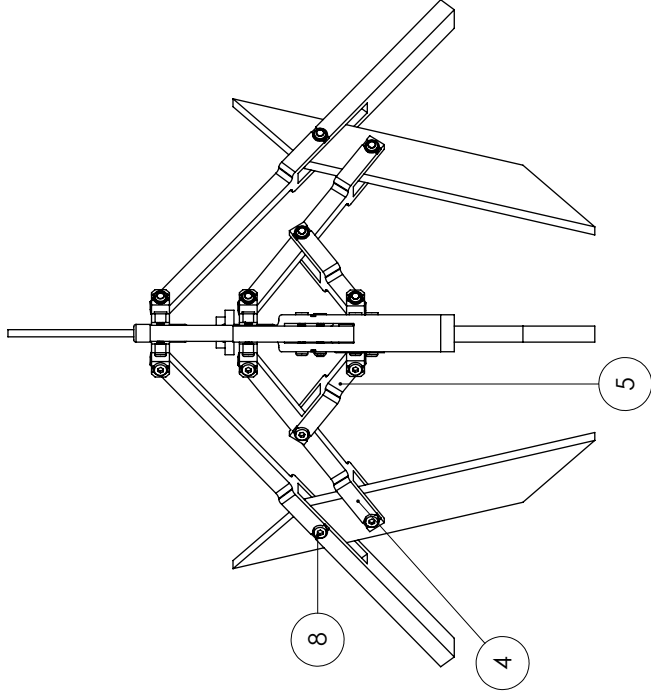
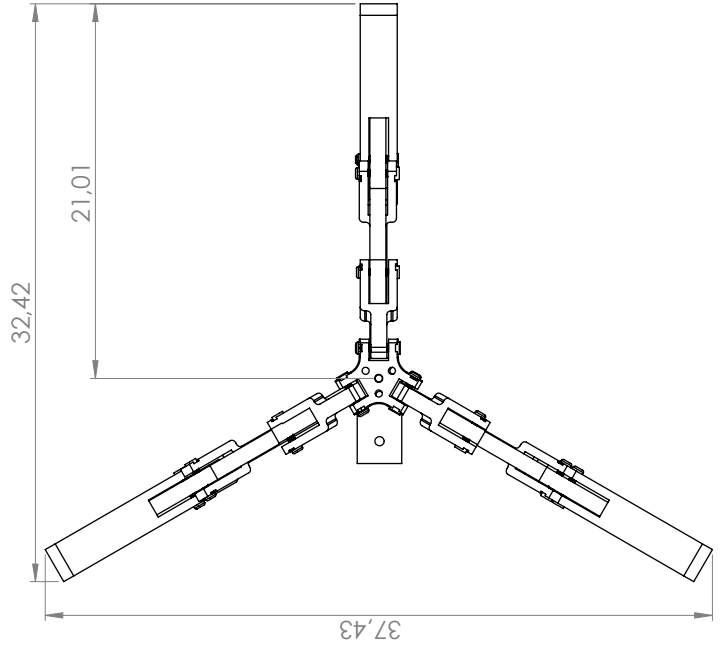
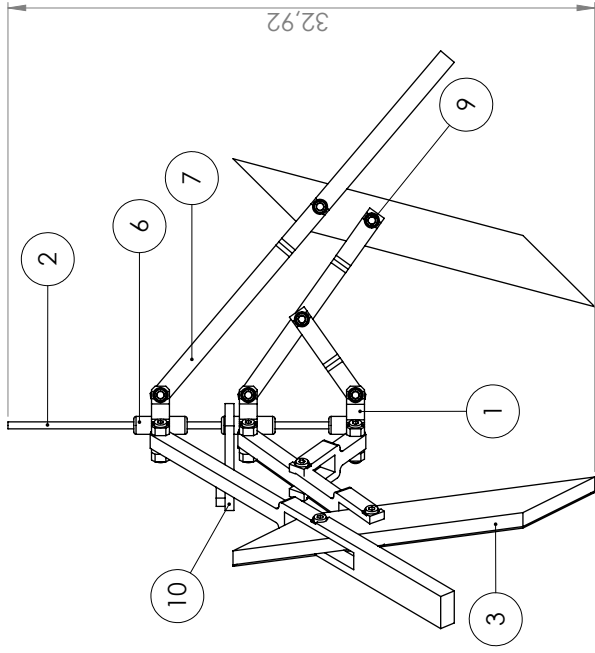


(e) Force top slider in unbalanced gripper minus force top slider in balanced gripper

(f) Force bottom slider in unbalanced gripper minus force bottom slider in balanced gripper

Figure 20: Mean actuation force comparison for different load cases

APPENDIX F
TECHNICAL DRAWINGS



ITEM NO.	PART NAME	QTY.
1	M4_wide_base	1
2	4 mm round steel bar	1
3	M4_wide_finger	3
4	M4_wide_Low_panto_L	3
5	M4_wide_Low_panto_s	3
6	M4_wide_slider	2
7	M4_wide_Upp_panto	3
8	M4x20 HEX CAP BOLT	18
9	M4 LOCK NUT	18
10	Act-slid_bracket	1

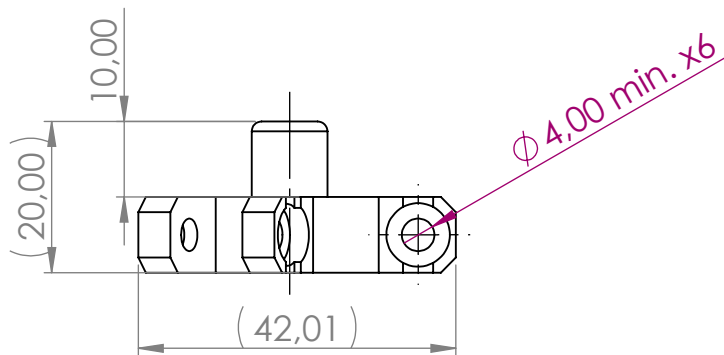
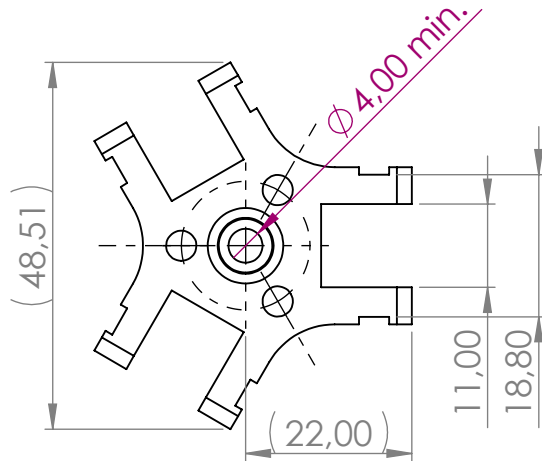
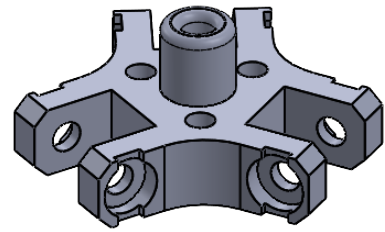
	units	scale	quantity	date	remark
material	mm	1:3	1	21-7-2024	This is a generic overview drawing of the assembly with BOM, indicated measurements are there to inform general size of total assembly as these can change with motion of the assembly
author	Rik Hofland - 4446070	group	ME MSC	mass	gr
			HTE MSD		

name **ASSY_M4_wide_joint_balanced_2DoF**

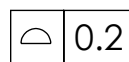
D:\Documenten\TU_Delft\Year_2\Solidworks\M4_size_wide_joint_balanced_2DoF\Drawings\

TU Delft Delft University of Technology

format **A3** drawing no. **1**

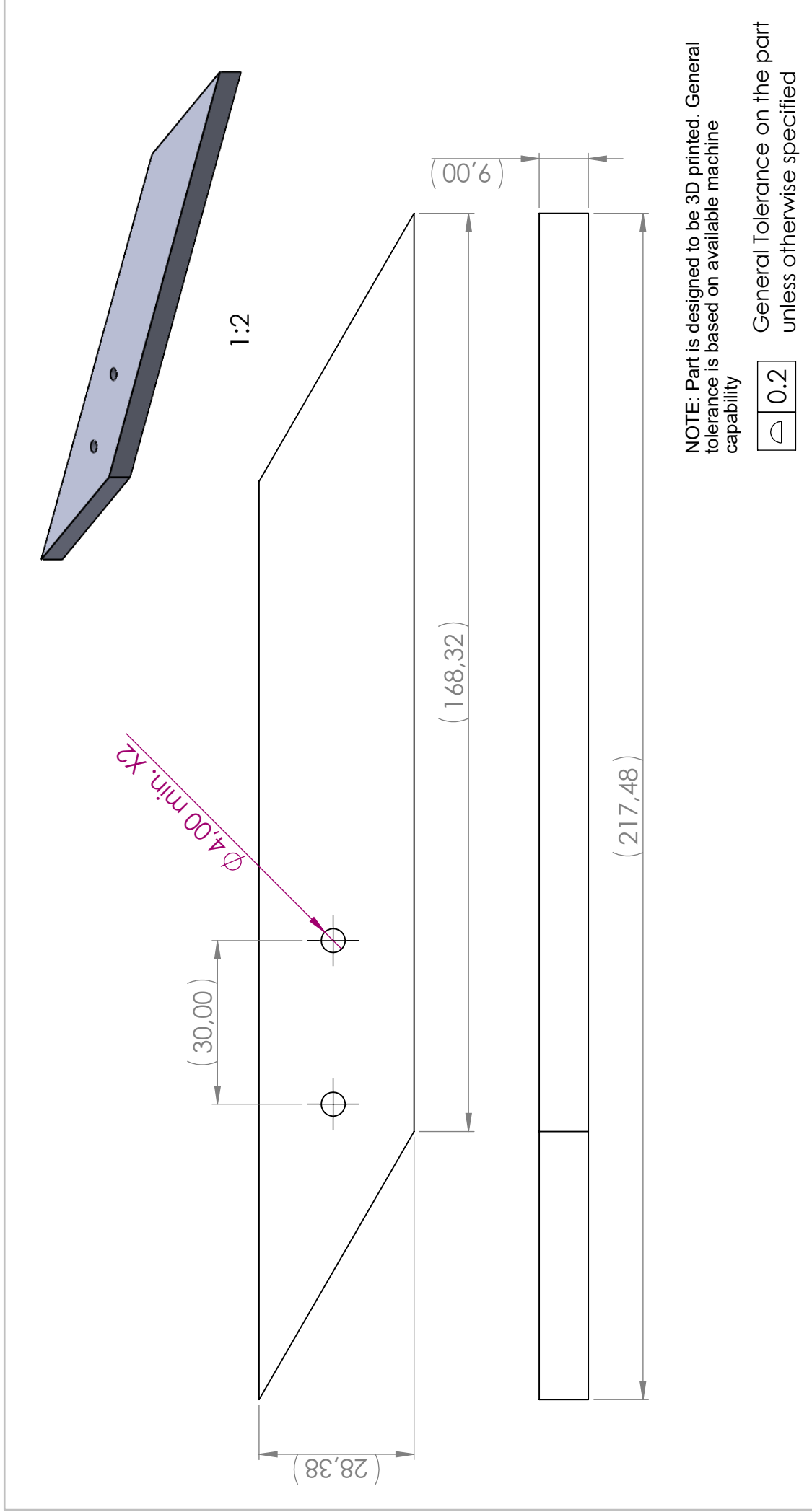


NOTE: Part is designed to be 3D printed. General tolerance is based on available machine capability

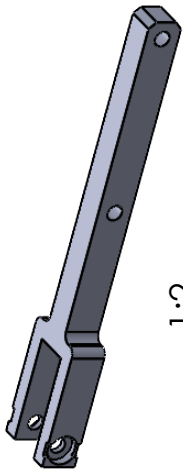


General Tolerance on the part unless otherwise specified

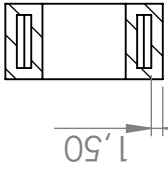
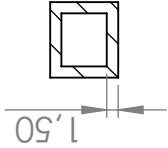
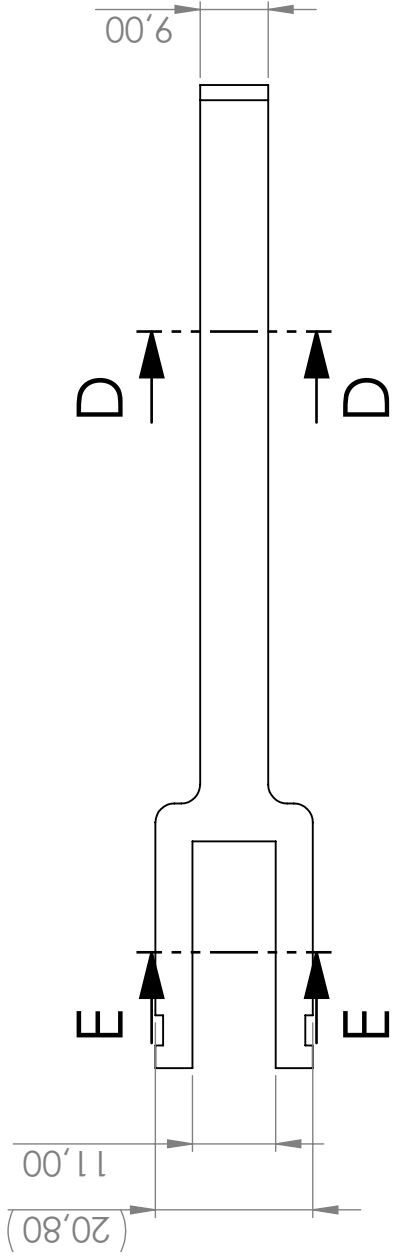
	units mm	scale 1:1	quantity 1	date 21-7-2024	remark
material			mass gr		 Delft University of Technology
author Rik Hofland - 4446070			group ME MSC HTE MSD		
name M4_wide_base				format A4	drawing no. 1
D:\Documenten\TU_Delft\Year_2\Solidworks\M4_size_wide_joint_balanced_2DoF\Drawings\					



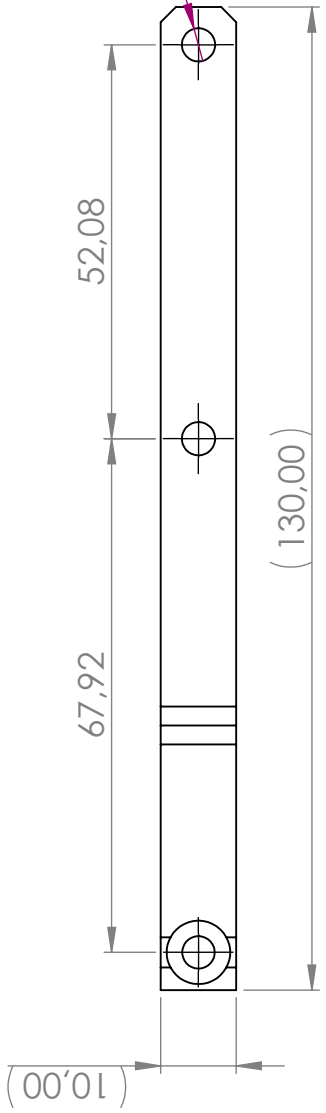
 Delft University of Technology	name M4_wide_finger		material author Rik Hofland - 4446070		quantity 3 scale 1:1 units mm		date 21-7-2024 mass format gr		remark <<remarks>>	
	D:\Documenten\TU_Delft\Year_2\Solidworks \M4_size_wide_joint_balanced_2DoF\Drawi ngs\		group ME MSC HTE MSD		drawing no. 1		format A4			



1:2



SECTION D-D SECTION E-E



NOTE: Part is designed to be 3D printed. General tolerance is based on available machine capability

\square 0.2

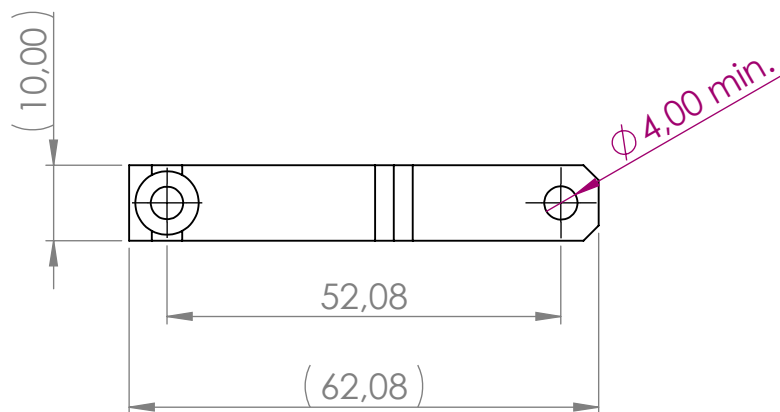
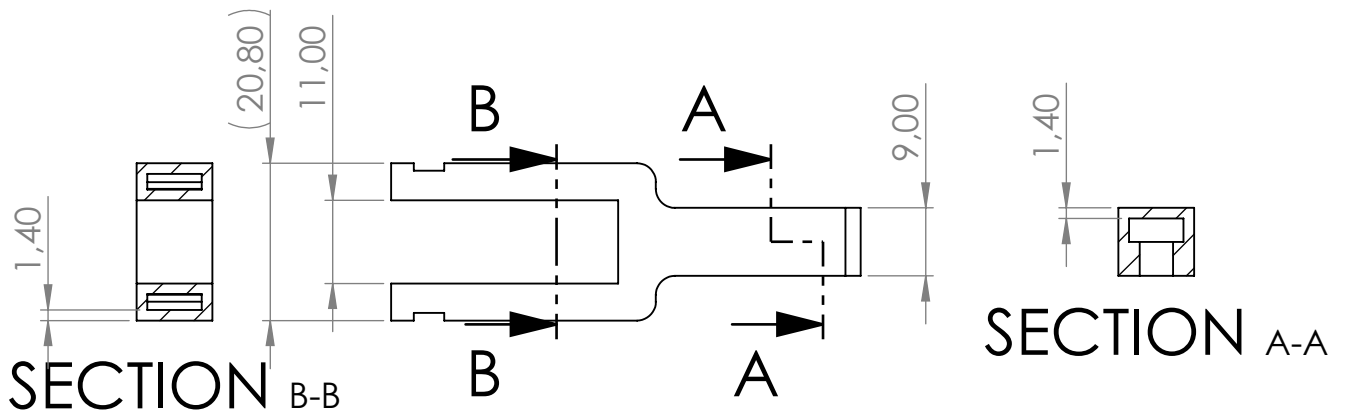
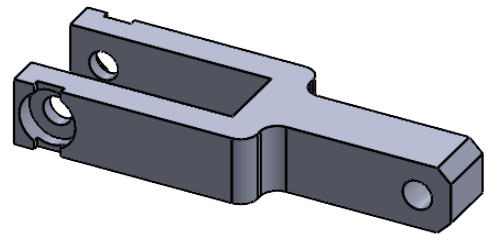
General Tolerance on the part unless otherwise specified

Delft University of Technology

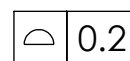
M4wide_Low_panto_L

D:\Documenten\TU_Delft\Year_2\Solidworks\M4_size_wide_joint_balanced_2DoFDrawi
ngs\

material	units	scale	quantity	date	remark
	mm	1:1	1	21-7-2024	<<remarks>>
author	group	format	mass	gr	
Rik Hofland - 4446070	ME MSC HTE MSD	A4			drawing no. 1

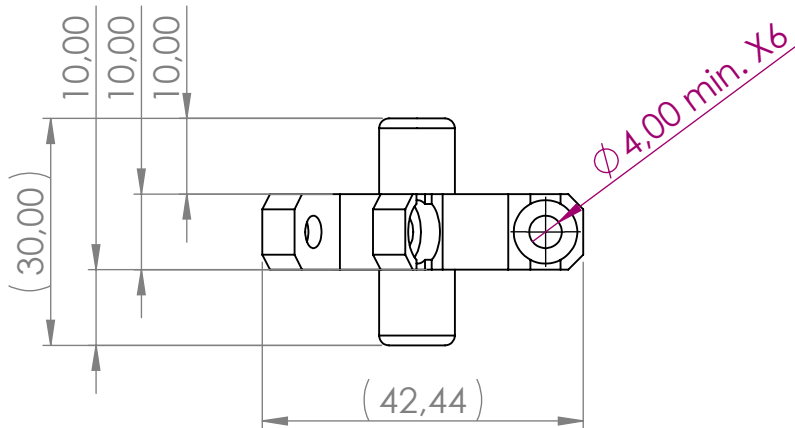
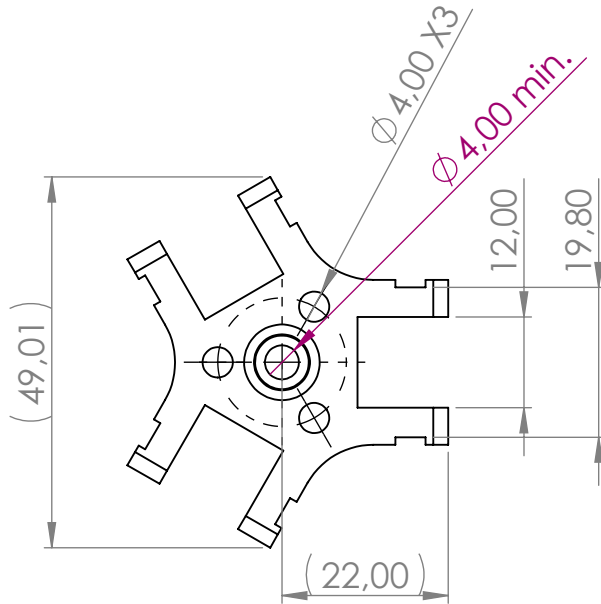
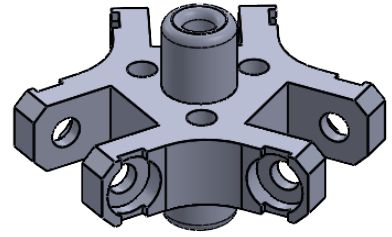


NOTE: Part is designed to be 3D printed. General tolerance is based on available machine capability

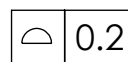


General Tolerance on the part unless otherwise specified

	units mm	scale 1:1	quantity 1	date 21-7-2024	remark <<remarks>>	
material			mass gr		 Delft University of Technology	
author Rik Hofland - 4446070			group ME MSC HTE MSD			
name M4_wide_Low_panto_s					format A4	drawing no. 1
D:\Documenten\TU_Delft\Year_2\Solidworks\M4_size_wide_joint_balanced_2DoF\Drawings\						



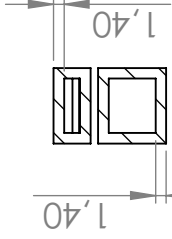
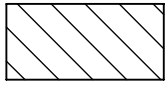
NOTE: Part is designed to be 3D printed. General tolerance is based on available machine capability



General Tolerance on the part unless otherwise specified

	units mm	scale 1:1	quantity 1	date 21-7-2024	remark <<remarks>>
material				mass	gr
author Rik Hofland - 4446070				group ME MSC HTE MSD	
name M4_wide_slider				format	drawing no.
				A4	1

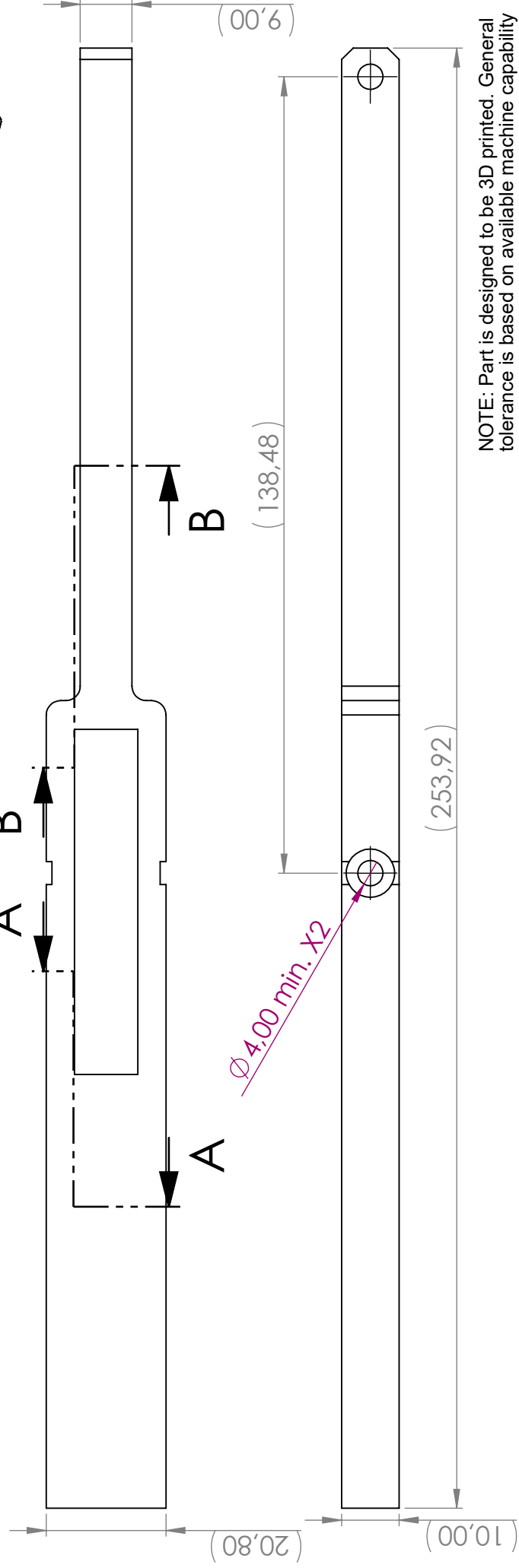




SECTION A-A

SECTION B-B

1:2



NOTE: Part is designed to be 3D printed. General tolerance is based on available machine capability

\square 0.2

General Tolerance on the part unless otherwise specified



material

scale

1:1

units

mm

quantity

1

date

21-7-2024

remark

<<remarks>>

group

ME MSC

HTE MSD

format

A4

drawing no.

1

author

Rik Hofland - 4446070

name

wide_Upp_panto

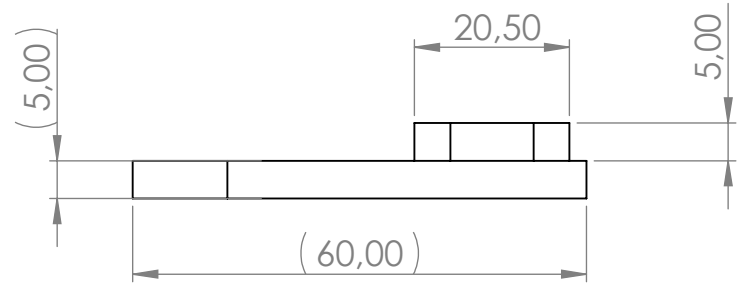
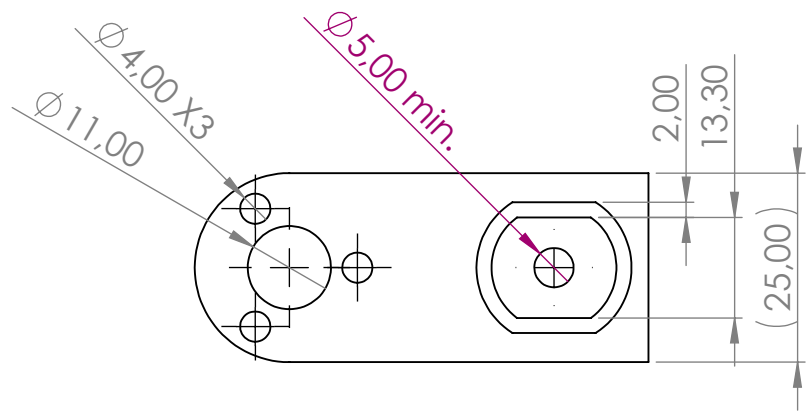
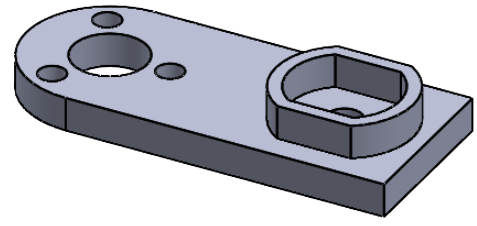
D:\Documenten\TU_Delft\Year_2\Solidworks

\M4_size_wide_joint_balanced_2DoFDrawi

ngs\

TU Delft

Delft University of Technology



NOTE: Part is designed to be 3D printed. General tolerance is based on available machine capability

\square 0.2 General Tolerance on the part unless otherwise specified

	units mm	scale 1:1	quantity 1	date 21-7-2024	remark <<remarks>>	
material			mass gr		 Delft University of Technology	
author Rik Hofland - 4446070			group ME MSC HTE MSD			
name Act-slid_bracket					format A4	drawing no. 1
D:\Documenten\TU_Delft\Year_2\Solidworks\M4_size_wide_joint_balanced_2DoF\Drawings\						

APPENDIX G
DESIGN DECISIONS

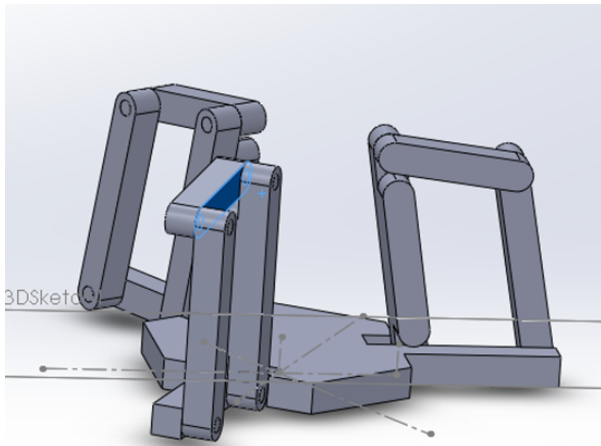
In order to come to a design for the gripper at first a comparison table was made to select suitable mechanisms for a balanced gripper design (Figure 21). In this table green is judged good, purple is depending on design, red is not possible or bad characteristic. The characteristics for both force and moment balance reflect if it would be possible to balance the mechanism. The criterion of rigidity is added because a gripper has to carry a load as well as its own mass hence a configuration that leads to a low rigidity when gripping an object is discarded. The column of interference with object refers to the motion the mechanism will make during the gripping movement. The gripper can not move through the to be gripped object. The lock in object column describes if the mechanism will be able to create a geometric locking design or if it will give a design depending on friction only. These columns together already make a hard selection in the proposed solutions as can be seen in the Yes/No column.

uneven fingers	coplanar	balans force	balance moment	rigidity	interference with object	lock in object	Y/N	function tracing speed single path	variable speed in out	variable size objects	#moving components to trace per finger	#total compon ents to trace 3 fingers	transmis sion angles
1	4bar prescribed motion (fixed to base)	green	green	green	purple	green	green	green	red	green	3	10	good
2	4 bar underdescribed motion (hinged at base)	green	red	green	purple	green	red	green	green	green	4	13	-
3	4bar actuating finger on rocker	green	green	green	purple	green	green	green	red	green	3	10	good
4	crank slider straight slider at base	green	green	green	red	green	red	green	green	green	2	7	-
5	crank slider straight, crank at base	green	green	green	red	red	red	green	green	red	3	10	-
6	crank slider curved slider at base	green	green	green	red	green	red	green	green	green	2	7	-
7	crank slider curved crank at base	green	green	green	green	red	red	green	green	red	3	10	-
8	crank slider both fixed straight	green	green	green	purple	green	green	green	green	purple	2	7	variing/good
9	crank slider both fixed curved	green	green	green	purple	green	green	green	green	purple	2	7	variing/good
10	scissor linkage	green	green	red	green	red	red	green	green	red	6	19	-
11	unfolding chain rigid linear actuated finger	green	red	purple	green	red	red	green	green	green	6	19	-
12	rigid rotating finger	green	green	green	green	green	green	red	green	green	1	4	-
13	curved scissor linkage	green	green	green	green	green	green	green	green	green	1	4	good
14	spatial curved slider crank at base	green	red	purple	purple	green	red	purple	green	red	2	7	-
15	spherical rotation around object	green	red	purple	purple	green	red	purple	purple	purple	4	13	-
16	straight line to object	green	green	purple	green	green	green	purple	purple	purple	2	7	n/a
17	extending to object (for instance with prismatic slide)	green	green	green	green	green	green	purple	purple	purple	1	4	n/a

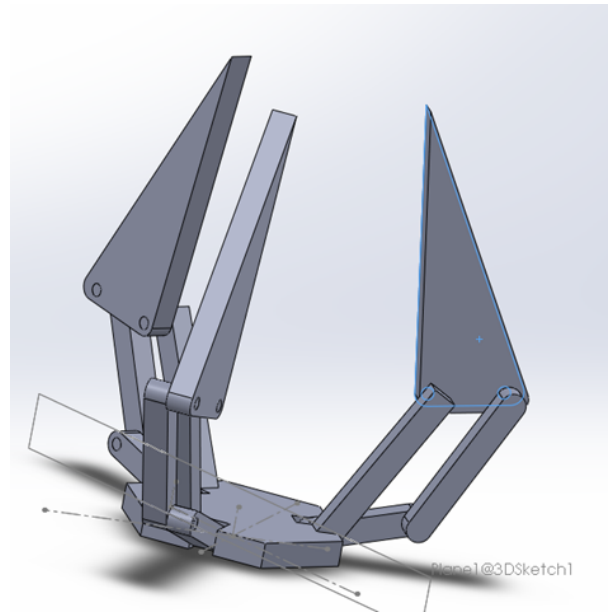
Figure 21: Evaluation of different mechanisms to use as base for gripper, in the table green is judged good, purple is depending on design, red is not possible or bad characteristic

In the second batch of columns a selection of other characteristics is evaluated per design with regards to extra features or complexities that are or can be added in a design with this type of mechanism. An example can be if the mechanism has a different movement velocity with the same actuations stroke in different parts of the stroke. This might be used to create a soft touch to the objects i.e. slowing down when closing in on the object and doing the fast bulk movement away from the object. The complexity of the design is gauged by the amount of components needed to make the mechanism work and balance it out.

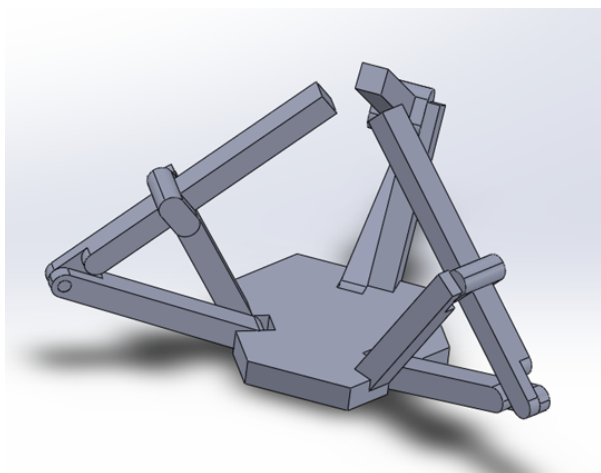
From this table four different mechanisms were chosen to work out further in CAD. The 4 bar fixed at base fully actuated Figure 22a, the 4 bar actuating finger on rocker Figure 22b, the crank slider both fixed relative to base Figure 22c, and the rigid rotating finger Figure 22d.



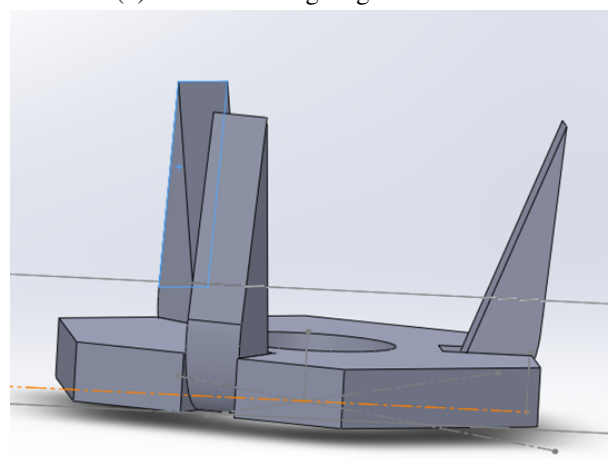
(a) 4 bar fixed at base fully actuated



(b) 4 bar actuating finger on rocker



(c) Crank slider both fixed relative to base

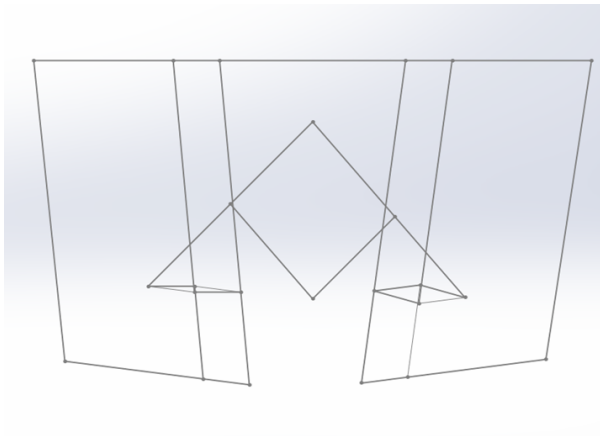


(d) Rigid rotating finger

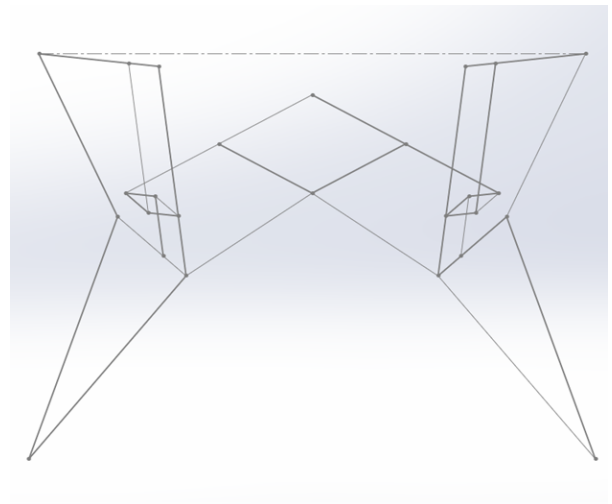
Figure 22: 4 designs chosen from mechanism table

After the mechanisms were drawn in CAD there was looked at adding mass tracing elements to the design to find the CoM of the mechanism where the base would have to be connected. In doing this it was clear that this design approach would lead to a very complex mechanism with a lot of elements (Figure 23).

A different approach was chosen where there was looked at the motion of the fingers. They were then connected to the base with inherent balanced mechanisms. In this phase again 4 different mechanism designs were generated where the fingers rotate around a fixed point Figure 24a, the finger only translates in horizontal direction by means of 2 linked pantographs Figure 24b, the fingers both rotate and translate attached to a single pantograph Figure 24c, and the fingers both rotate and translate attached to 2 independent pantographs Figure 24d.

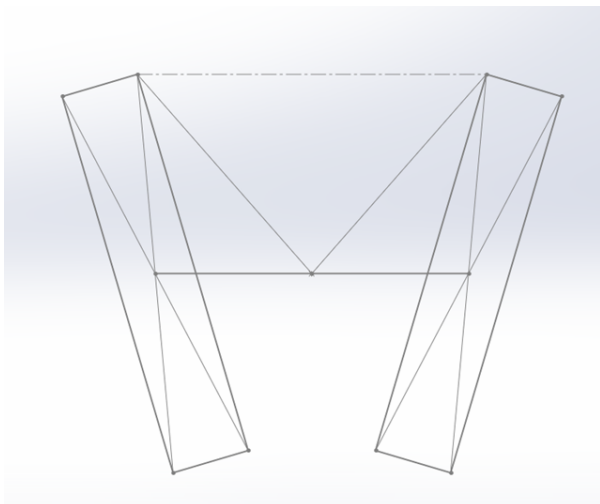


(a) 4 bar fixed at base fully actuated with mass tracing elements 2D

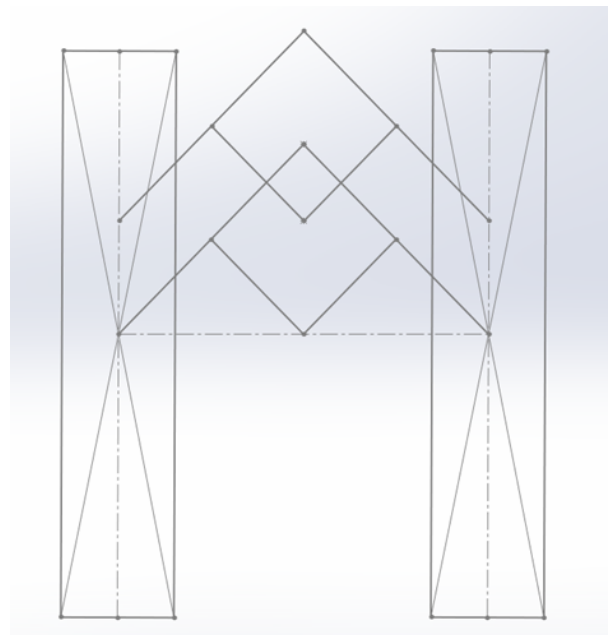


(b) 4 bar actuating finger on rocker with mass tracing elements 2D

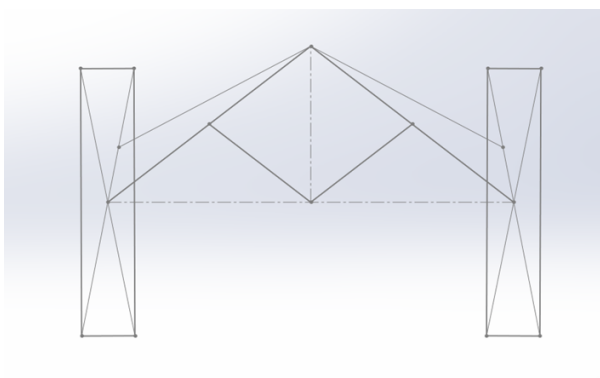
Figure 23: Mass tracing elements in both selected 4 bar mechanisms



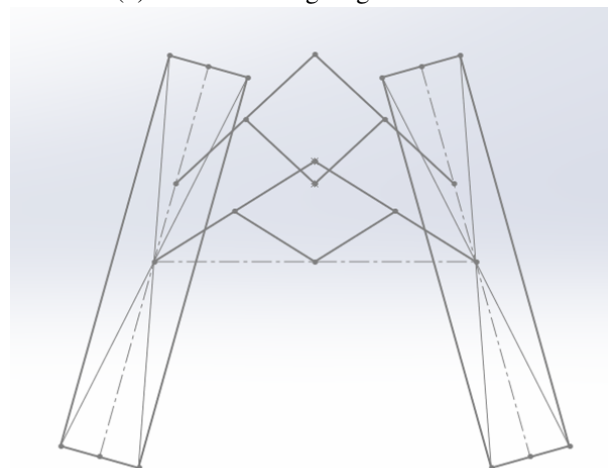
(a) 4 bar fixed at base fully actuated



(b) 4 bar actuating finger on rocker



(c) Crank slider both fixed relative to base



(d) Rigid rotating finger

Figure 24: 4 designs chosen from finger motion attached with inherent balanced elements

In comparing the four different designs it was seen that the gripper with only rotating fingers could have an ideal grip for only one size objects and in extending this concept to multi-fingered 3D designs it would get complex gearing systems to not have to rely on equal rotation from actuator control which is not mechanical balance. The translating gripper can grip different sized objects, but it can only do so by a pinch/friction grip and will never geometrically constrain the objects. The grippers combining two motions can both achieve the geometrical locking. However, the version with the single pantograph only has an ideal grip for 1 size objects where as the double pantograph version has a range of objects it can pick up with the ideal geometric grip. The counter advantage of the single pantograph gripper is its simplicity. In the end there was chosen to go for the size range rather than the simpler mechanism. This would lead to a larger array of possible use cases which was preferred because no specific case was specified and hence the gripper could not be optimised for such a case.

APPENDIX H
MATLAB CODE POSITION SIMULATION

```
1 clear all
2 close all
3 %{
4
5 phi1 =      0;
6 phi2 =  2.0349;
7 phi3 =  1.6873;
8 phi4 =  3.4481;
9 phi5 =  1.4543;
10 phi6 =      0;
11 phi7 =      0;
12 phi8 = -2.0349;
13 phi9 = -1.6873;
14 phi10 = -3.4481;
15 phi11 = -1.4543;
16 phid1 =      0;
17 phid2 =      0;
18 phid3 =      0;
19 phid4 =      0;
20 phid5 =      0;
21 phid6 =      0;
22 phid7 =      0;
23 phid8 =      0;
24 phid9 =      0;
25 phid10 =      0;
26 phid11 =      0;
27
28
29 %CoM's alle verschillende bodies
30 Cx1 = x1;
31 Cy1 = y1 - com1;
32 Cx2 = x2 -(16/2) -com2*cos(phi2);
33 Cy2 = y2 -com2*sin(phi2) -y7;
34 Cx3 = x3 -(16/2) -com3*cos(phi3);
35 Cy3 = y3 -com3*sin(phi3) -y6;
36 Cx4 = x4 -com4x*cos(phi4) -13*cos(phi3) -(16/2);
37 Cy4 = y4 -com4y*sin(phi4) -13*sin(phi3) -y6;
38 Cx5 = x5 -(15/2)*cos(phi5) -(16/2);
39 Cy5 = y5 -(15/2)*sin(phi5) - 5*10-3;
40 Cx6 = x6;
41 Cy6 = y6 -l_act1;
42 Cx7 = x7;
43 Cy7 = y7 -l_act2;
44 Cx8 = x8 -(16/2) -com2*cos(phi8);
45 Cy8 = y8 -com2*sin(phi8) -y7;
46 Cx9 = x9 -(16/2) -com3*cos(phi9);
47 Cy9 = y9 -com3*sin(phi9) -y6;
48 Cx10 = x10 -com4x*cos(phi10) -19*cos(phi9) -(16/2);
49 Cy10 = y10 -com4y*sin(phi10) -19*sin(phi9) -y6;
```

```

50 Cx11 = x11 - (l11/2)*cos(phi11) - (l6/2);
51 Cy11 = y11 - (l11/2)*sin(phi11) - 5*10^-3;
52
53 % EoM_Balanced_2DoF(phi2,phi3,phi4,phi5,phi8,phi9,phi10,phi11,phid2,phid3
    ,phid4,phid5,phid8,phid9,phid10,phid11)
54 %}
55 clc
56 %%
57 %masses kg
58 m1 = 12.70604*10^-3;
59 m2 = 51.75832*10^-3;
60 m3 = 34.19995*10^-3;
61 m4 = 101.17311*10^-3;
62 m5 = 18.74735*10^-3;
63 m6 = 3.63381*10^-3;
64 m7 = m6;
65 m8 = m2;
66 m9 = m3;
67 m10 = m4;
68 m11 = m5;
69
70 %inertias kg*m^2
71 I1 = 460636.56*10^-9;
72 I2 = 177590.40*10^-9;
73 I3 = 156700.05*10^-9;
74 I4 = 300239.04*10^-9;
75 I5 = 11764.35*10^-9;
76 I6 = 3371.28*10^-9;
77 I7 = I6;
78 I8 = I2;
79 I9 = I3;
80 I10 = I4;
81 I11 = I5;
82
83 %lengths m
84 l1 = 260*10^-3;
85 l2 = 2*92.32*10^-3;
86 l3 = 2*75*10^-3;
87 %l4 = 240*10^-3;
88 l4 = 2*30*10^-3;
89 l6 = 24*10^-3;
90 l7 = l6;
91 l8 = l2;
92 l9 = l3;
93 l10 = l4;
94
95 %specific values for balance calculations
96 m2_link = 14.030*10^-3; %weight of link 2 without counterweight
97 Com2_link = 127.5*10^-3; %CoM position of link 2 measured from pivot with
    4
98 Com3_link = 107.5*10^-3;
99

```

```

100
101 %%
102 %calculate the length of counterweight at part 2
103 %x = ;
104 y_counter = 30*10^-3;
105 z_counter = 10*10^-3;
106 btwn_length = 40*10^-3;
107 square_stock = 10*10^-3;
108
109 M_26 = (m2_link/1000)*Com2_link+12*(m6/1000)/2;%the divide by 1000 is to
    be able to compare volumes and not masses, other option is to multiply
    volumes by density for different densities
110 %side2 = 2*10*10*tussen*tussen/2+ 2*x*y*z*(x/2+tussen);
111 xcounter1 = -btwn_length +sqrt(btwn_length^2-4*0.5*-((M_26-(2*
    square_stock*square_stock*btwn_length*btwn_length/2)))/(2*y_counter*
    z_counter));
112 xcounter2 = -btwn_length -sqrt(btwn_length^2-4*0.5*-((M_26-(2*
    square_stock*square_stock*btwn_length*btwn_length/2)))/(2*y_counter*
    z_counter));
113 xcounter = max(xcounter1,xcounter2)
114 %bal = side1-side2;
115
116 %calculate the length of the finger
117 offset1 = 80*10^-3;
118 %x = 248.9602;
119 y_finger = 40*10^-3;
120 z_finger = 10*10^-3;
121
122 Upp_panto = ((m2/1000)+(m6/1000)/2)*offset1;%side1
123 %side2 = x*y*z*(x/2-5-offset1);
124
125 x_finger1 = (5*10^-3+offset1)+sqrt((5*10^-3+offset1)^2-4*0.5*-((Upp_panto
    )/(y_finger*z_finger)));
126 x_finger2 = (5*10^-3+offset1)-sqrt((5*10^-3+offset1)^2-4*0.5*-((Upp_panto
    )/(y_finger*z_finger)));
127 x_finger = max(x_finger1,x_finger2)
128 %bal = side1-side2
129
130 %%
131 %CoM specific lengths
132 l_com1 = 95.56*10^-3;
133 l_com2 = 12+(m7/2*12)/m2;%141.64*10^-3;
134 l_com3 = (0*(m7/2)+CoM3_link*m3+(m2+m6/2+m4)*13)/(m2+m6/2+m4+m3+m7/2);
135 % l_com4x = 0;%0.17*10^-3;
136 % l_com4y = 0;%0.02*10^-3;
137 l_com4 = (14*(m2+m6/2))/m4;%from CoM of m2+m6/2 and m4 which needs to be
    at the foot of the pantograph
138 %dx4hole = 75.15*10^-3;
139 %dy4hole = 9.02*10^-3;
140 l_com8 = l_com2;%141.64*10^-3;
141 l_com9 = l_com3;
142

```

```

143 %calculate length of small pantograph arm for balance
144 l5 = (0*(m7/2)+l_com3*m3+(m2+m6/2+m4)*l3)/(m2+m4+m3+m8+m6+m10+m9+m7+m11
      /2)%107.5*10^-3;
145 l11 = l5;
146
147 % %m2+m6/2+m4+m3+m7/2
148 %
149 % lCoM3 = (0*(m7/2)+l_com3*m3+(m2+m6/2+m4)*l3)/(m2+m6/2+m4+m3+m7/2);
150 % a1 = (0*(m7/2)+l_com3*m3+(m2+m6/2+m4)*l3)/(m2+m4+m3+m8+m6+m10+m9+m7+m11
      /2);
151
152 %%
153 l_A1 = linspace(10*10^-3, 130*10^-3);
154 l_A2 = linspace(70*10^-3, 200*10^-3);
155
156 x = zeros(length(l_A1),11);
157 y = zeros(length(l_A1),11);
158 phi = zeros(length(l_A1),11);
159
160 for i = 1:length(l_A1)
161
162     x(i,1) = 0;
163     y(i,1) = l_com1;
164     phi(i,1) = 0;
165
166
167
168     x(i,3) = -l6/2-l_com3*sin(pi-acos(l_A1(i)/(2*15)));
169     y(i,3) = l_A1(i)+l_com3*cos(pi-acos(l_A1(i)/(2*15)));
170     phi(i,3) = pi-acos(l_A1(i)/(2*15));
171
172     li = sqrt(l3^2+(l_A2(i)-l_A1(i))^2-2*l3*(l_A2(i)-l_A1(i))*cos(
      phi(i,3)));
173     phi3li = acos(-((l_A2(i)-l_A1(i))^2+li^2+l3^2)/(2*li*l3));
174     phili4 = acos(-((l2^2)+li^2+l4^2)/(2*li*l4));
175
176     phi(i,4) = phi(i,3)-pi+phi3li+phili4;
177     x(i,4) = -l6/2-l3*sin(phi(i,3))+l_com4*sin(phi(i,4));
178     y(i,4) = l_A1(i)+l3*cos(phi(i,3))-l_com4*cos(phi(i,4));
179
180     %balance term
181     phi(i,2) = pi - atan(-((l6/2)+x(i,4)-(l_com4+l4)*sin(phi(i,4)))/(
      l_A2(i)-(y(i,4)+(l_com4+l4)*cos(phi(i,4)))));
182     x(i,2) = -l6/2-l_com2*sin(phi(i,2));
183     y(i,2) = l_A2(i)+l_com2*cos(phi(i,2));
184
185     x(i,5) = -l6/2-(l5/2)*sin(acos(l_A1(i)/(2*15)));
186     y(i,5) = l_A1(i)/4;
187     phi(i,5) = acos(l_A1(i)/(2*15));
188     x(i,6) = 0;
189     y(i,6) = l_A1(i);
190     phi(i,6) = 0;
191     x(i,7) = 0;

```

```

191     y(i,7)      = l_A2(i);
192     phi(i,7)   = 0;
193
194     x(i,9)      = 16/2-l_com9*sin(-pi + acos(l_A1(i)/(2*l11)));
195     y(i,9)      = l_A1(i) +l_com9*cos(-pi+acos(l_A1(i)/(2*l11)));
196     phi(i,9)    = -pi + acos(l_A1(i)/(2*l11));
197
198
199     li2         = sqrt(19^2+(l_A2(i)-l_A1(i))^2-2*19*(l_A2(i)-l_A1(i))*cos(
200         phi(i,9)));
201     phi9li      = acos(-((l_A2(i)-l_A1(i))^2) + li2^2 + 19^2) / (2*li2*19)
202         ;
203     phili10     = acos(-(18^2) + li2^2 + 110^2)/(2*li2*110));
204
205     phi(i,10)   = phi(i,9)+pi - phi9li -phili10;
206     x(i,10)     = 16/2-19*sin(phi(i,9))+l_com4*sin(phi(i,10));
207     y(i,10)     = l_A1(i)+19*cos(phi(i,9))-l_com4*cos(phi(i,10));
208
209     phi(i,8)    = -pi+atan((-16/2)+x(i,10)-(110+l_com4)*sin(phi(i,10)))/(
210         l_A2(i) - (y(i,10)+(110+l_com4)*cos(phi(i,10))));
211     x(i,8)      = 16/2-l_com8*sin(phi(i,8));
212     y(i,8)      = l_A2(i)+l_com8*cos(phi(i,8));
213
214     x(i,11)     = 16/2 + (l11/2)*sin(acos(l_A1(i)/(2*l11)));
215     y(i,11)     = l_A1(i)/4;
216     phi(i,11)   = -acos(l_A1(i)/(2*l11));
217 end
218
219 %
220 % dl = zeros(100,1);
221 % for i = 1:100
222 % dl(i) = sqrt((x(i,10)+110*sin(phi(i,10))-16/2)^2+(l_A2(i) - (y(i,10)+
223     110*cos(phi(i,10))))^2);
224 % end
225 %
226 %%
227 % close all
228 % plot([x(1,3)+13/2*sin(phi(1,3))    x(1,3)-13/2*sin(phi(1,3))] , [y
229     (1,3)-13/2*cos(phi(1,3))    y(1,3)+13/2*cos(phi(1,3))], 'LineWidth',5)
230 % hold on
231 % plot([x(1,2)+12/2*sin(phi(1,2))    x(1,3)-12/2*sin(phi(1,2))] , [y
232     (1,2)+12/2*cos(phi(1,2))    y(1,2)-12/2*cos(phi(1,2))], 'LineWidth',5)
233 % plot([x(1,5)+15/2*sin(phi(1,5))    x(1,5)-15/2*sin(phi(1,5))] , [y
234     (1,5)-15/2*cos(phi(1,5))    y(1,5)+15/2*cos(phi(1,5))], 'LineWidth',5)
235 % plot([x(1,8)+18/2*sin(phi(1,8))    x(1,8)-18/2*sin(phi(1,8))] , [y
236     (1,8)+18/2*cos(phi(1,8))    y(1,8)-18/2*cos(phi(1,8))], 'LineWidth',5)
237 % plot([x(1,9)+19/2*sin(phi(1,9))    x(1,9)-19/2*sin(phi(1,9))] , [y
238     (1,9)-19/2*cos(phi(1,9))    y(1,9)+19/2*cos(phi(1,9))], 'LineWidth',5)
239 % plot([x(1,11)+111/2*sin(phi(1,11)) x(1,11)-111/2*sin(phi(1,11))] , [y
240     (1,11)-111/2*cos(phi(1,11)) y(1,11)+111/2*cos(phi(1,11))], 'LineWidth

```

```

    ',5)
233 % plot ([x(1,6)+16/2          x(1,6)-16/2]          , [y
    (1,6)          y(1,6)], 'LineWidth',5)
234 % plot ([x(1,7)+17/2          x(1,7)-17/2]          , [y
    (1,7)          y(1,7)], 'LineWidth',5)
235 % plot ([x(1,4)          x(1,4)+14*sin(phi(1,4))]          , [y
    (1,4)          y(1,4)+14*cos(phi(1,4))], 'LineWidth',5)
236 % plot ([x(1,10)          x(1,10)+110*sin(phi(1,10))]          , [y
    (1,10)          y(1,10)+110*cos(phi(1,10))], 'LineWidth',5)
237 % plot ([x(1,1)          x(1,1)]          , [y
    (1,1)-1_com1          y(1,1)+11-1_com1], 'LineWidth',5)
238 % legend('3','2','5','8','9','11','6','7','4','10','1')
239 % for i = 1:11
240 % plot(x(1,i), y(1,i), '*')
241 % end
242
243 figure(1)
244
245 for j = 5:5:length(l_A1)
246     plot ([x(j,3)+1_com3*sin(phi(j,3))          x(j,3)-(13-1_com3)*
    sin(phi(j,3))]          , [y(j,3)-1_com3*cos(phi(j,3))          y(j
    ,3)+(13-1_com3)*cos(phi(j,3))], 'LineWidth',5)
247     hold on
248     title(['step:', num2str(j)])
249     plot ([x(j,2)+1_com2*sin(phi(j,2))          x(j,2)-(12-1_com2)*sin(phi(
    j,2))]          , [y(j,2)-1_com2*cos(phi(j,2))          y(j,2)+(12-1_com2)*cos
    (phi(j,2))], 'LineWidth',5)
250     plot ([x(j,5)+15/2*sin(phi(j,5))          x(j,5)-15/2*sin(phi(j
    ,5))]          , [y(j,5)-15/2*cos(phi(j,5))          y(j,5)+15/2*cos(
    phi(j,5))], 'LineWidth',5)
251     plot ([x(j,8)+1_com8*sin(phi(j,8))          x(j,8)-(18-1_com8)*sin(phi(
    j,8))]          , [y(j,8)-1_com8*cos(phi(j,8))          y(j,8)+(18-1_com8)*cos
    (phi(j,8))], 'LineWidth',5)
252     plot ([x(j,9)+1_com9*sin(phi(j,9))          x(j,9)-(19-1_com9)*
    sin(phi(j,9))]          , [y(j,9)-1_com9*cos(phi(j,9))          y(j
    ,9)+(19-1_com9)*cos(phi(j,9))], 'LineWidth',5)
253     plot ([x(j,11)+111/2*sin(phi(j,11))          x(j,11)-111/2*sin(phi(
    j,11))]          , [y(j,11)-111/2*cos(phi(j,11))          y(j,11)+111/2*cos
    (phi(j,11))], 'LineWidth',5)
254     plot ([x(j,6)+16/2          x(j,6)-16/2]
    , [y(j,6)          y(j,6)],
    'LineWidth',5)
255     plot ([x(j,7)+17/2          x(j,7)-17/2]
    , [y(j,7)          y(j,7)],
    'LineWidth',5)
256     plot ([x(j,4)          x(j,4)-(14+1_com4)*sin
    (phi(j,4))]          , [y(j,4)          y(j,4)+(14+1_com4
    )*cos(phi(j,4))], 'LineWidth',5)
257     plot ([x(j,10)          x(j,10)-(110+1_com4)*
    sin(phi(j,10))]          , [y(j,10)          y(j,10)
    +(110+1_com4)*cos(phi(j,10))], 'LineWidth',5)

```

```

258     plot([x(j,1)                                x(j,1)]
          , [y(j,1)-l_com1                        y(j
          ,1)+l1-l_com1], 'LineWidth',5)
259     legend('3', '2', '5', '8', '9', '11', '6', '7', '4', '10', '1')
260     xlim([-300,300]*10^-3)
261     ylim([-100,300]*10^-3)
262     set(gcf, 'Position', [100,100,1000,700])
263     pause(0.000001)
264     hold off
265 end
266 for i = 1:11
267     hold on
268     plot(x(length(l_A1),i), y(length(l_A1),i), '*')
269 end
270
271 %%
272 M = [m2 m3 m4 m5 m6 m7 m8 m9 m10 m11].';%[0 0 0 m4 0 0 0 0 0 m10 0].';%
      %1 weg gelaten want die beweegt niet
273 CoM_x = zeros(length(l_A1),1);
274 CoM_y = zeros(length(l_A1),1);
275
276 for j = 1:length(l_A1)
277     CoM_x(j) = x(j,2:11)*M/sum(M);
278     CoM_y(j) = y(j,2:11)*M/sum(M);
279 end
280 figure
281 plot(1:length(l_A1),CoM_x);
282 title('change in CoM position x-direction')
283
284
285 figure
286 plot(1:length(l_A1),CoM_y);
287 title('change in CoM position y-direction')
288 % ylim([-10,10]*10^-3)
289 %%
290 %
291 % t = 20*10^-2;
292 % dt = t/length(l_A1);
293 %
294 % v_x = zeros(length(l_A1),11);
295 % a_x = zeros(length(l_A1),11);
296 % v_y = zeros(length(l_A1),11);
297 % a_y = zeros(length(l_A1),11);
298 % v_phi = zeros(length(l_A1),11);
299 % a_phi = zeros(length(l_A1),11);
300 %
301 %
302 % for n = 2:100
303 %     v_x(n,:) = (x(n,:)-x(n-1,:))/dt;
304 %     v_y(n,:) = (y(n,:)-y(n-1,:))/dt;
305 %     v_phi(n,:) = (phi(n,:)-phi(n-1,:))/dt;
306 % end

```

```

307 % for n = 3:100
308 %     a_x(n,:) = (x(n,:)-2*x(n-1,:)+x(n-2,:))/dt^2;
309 %     a_y(n,:) = (y(n,:)-2*y(n-1,:)+y(n-2,:))/dt^2;
310 %     a_phi(n,:) = (phi(n,:)-2*phi(n-1,:)+phi(n-2,:))/dt^2;
311 % end
312 %
313 % I = [I2 I3 I4 I5 I6 I7 I8 I9 I10 I11];%1 weg gelaten want die beweegt
      niet
314 %
315 % F_x = a_x.*M.';
316 % F_y = a_y.*M.';
317 % F_phi = a_phi.*I;
318 %
319 % figure
320 % subplot(3,1,1)
321 % plot(1:length(l_AB),v_x)
322 % title('x velocities of bodies')
323 % subplot(3,1,2)
324 % plot(1:length(l_AB),v_y)
325 % title('y velocities of bodies')
326 % subplot(3,1,3)
327 % plot(1:length(l_AB),v_phi)
328 % title('moments velocities of bodies')
329 % legend('1','2','3','4','5','6','7','8','9','10','11')
330 %
331 % figure
332 % subplot(3,1,1)
333 % plot(1:length(l_A1),F_x)
334 % title('x Forces on bodies')
335 % subplot(3,1,2)
336 % plot(1:length(l_A1),F_y)
337 % title('y Forces on bodies')
338 % subplot(3,1,3)
339 % plot(1:length(l_A1),F_phi)
340 % title('moments on bodies')
341 % legend('1','2','3','4','5','6','7','8','9','10','11')
342 %
343 % figure
344 % subplot(3,1,1)
345 % plot(1:length(l_A1),a_x)
346 % title('x accelerations of bodies')
347 % subplot(3,1,2)
348 % plot(1:length(l_A1),a_y)
349 % title('y accelerations of bodies')
350 % subplot(3,1,3)
351 % plot(1:length(l_A1),a_phi)
352 % title('rotation accelerations of bodies')
353 % legend('1','2','3','4','5','6','7','8','9','10','11')
354 %

```

APPENDIX I
MATLAB CODE SPACAR SIMULATION

```
1 %% 2 DOF basic pantograph
2 clear all
3 close all
4
5 addpath('D:\Documenten\TU_Delft\Year_2\Spacar')
6
7 %% known parameters
8 %masses kg
9 m1 = 1*10^-3;
10 %m2 = 20.14787030*10^-3;
11 m3 = 9.28964478*10^-3;
12 % m4 = 20.01308796967819*10^-3;%.92010620*10^-3;
13 m5 = 4.90762524*10^-3;
14 m6 = 9.36522987*10^-3;
15 m7 = m6;
16 %m8 = m2;
17 m9 = m3;
18 % m10 = m4;
19 m11 = m5;
20 m_joint = 3.778*10^-3;
21
22 %lengths m
23 l1 = 200*10^-3;
24 l2 = 138.48*10^-3;
25 l3 = 120*10^-3;
26 %l4 = 240*10^-3;
27 l4 = 30*10^-3;
28 l6 = 15*10^-3;
29 l7 = l6;
30 l8 = l2;
31 l9 = l3;
32 l10 = l4;
33 l_j2e = 5*10^-3;
34
35 %specific values for balance calculations
36 m2_link = 9.76369795*10^-3; %weight of link 2 without counterweight
37 CoM2_link = 12-78.95074887*10^-3-l_j2e; %CoM position of link 2 measured
    from pivot with 4
38 CoM3_link = 13-69.13293431*10^-3-l_j2e;
39 CoM5_link = 31.85564927*10^-3-l_j2e;
40
41
42 %material
43 density = 1240;
44
45 n_arms = 3; %number of arms/fingers
46
47 %% Conversion from without to with joints
48 m5j = m5+m_joint;
```

```

49 m11j = m5j;
50
51 m6j = m6+n_arms*m_joint;
52 m7j = m6j;
53
54 CoM3_link_j = (m3*CoM3_link+l3*m_joint)/(m3+m_joint);
55 CoM9_link_j = CoM3_link_j;
56 m3j = m3+m_joint;
57 m9j = m3j;
58
59
60 %% kinematics
61 %calculate the length of counterweight at part 2
62 %x = ;
63 y_counter = 20.8*10^-3;
64 z_counter = 10*10^-3;
65 btwn_length = 30*10^-3;
66 square_stock_1 = 10*10^-3;
67 square_stock_2 = 4.9*10^-3;
68
69 M_26 = (m2_link/density)*CoM2_link+l2*((m6j)/density)/n_arms;%the divide
    by 1000 is to be able to compare volumes and not masses, other option
    is to multiply volumes by density for different densities
70 %side2 = 2*10*10*tussen*tussen/2+ 2*x*y*z*(x/2+tussen);
71 x_counter1 = -(l_j2e+btwn_length)+sqrt((l_j2e+btwn_length)^2-4*(1/2)*-((
    l2*m7j/n_arms + m2_link*CoM2_link - 2*btwn_length*square_stock_1*
    square_stock_2*density*(l_j2e+btwn_length/2))/(y_counter*z_counter*
    density)));
72 x_counter2 = -(l_j2e+btwn_length)-sqrt((l_j2e+btwn_length)^2-4*(1/2)*-((
    l2*m7j/n_arms + m2_link*CoM2_link - 2*btwn_length*square_stock_1*
    square_stock_2*density*(l_j2e+btwn_length/2))/(y_counter*z_counter*
    density)));
73 x_counter = max(x_counter1,x_counter2);
74 %bal = side1-side2;
75 check_upp_bal = m2_link*CoM2_link+m7j/n_arms*l2-(l_j2e+btwn_length/2)*2*
    btwn_length*square_stock_1*square_stock_2*density-(l_j2e+btwn_length+
    x_counter/2)*x_counter*y_counter*z_counter*density;
76
77 m2 = m2_link+2*btwn_length*square_stock_1*square_stock_2*density+
    x_counter*y_counter*z_counter*density;
78 m8 = m2;
79 %calculate the length of the finger
80 y_finger = 20*10^-3;
81 z_finger = 9*10^-3;
82
83 % Upp_panto = ((m2/density)+(m7j/2/density)+(m_joint/density))*l4;%side1
84 %side2 = x*y*z*(x/2-5-l4);
85
86
87 x_finger1 = (l4+l_j2e)+sqrt((l4+l_j2e)^2-4*(1/2)*-((m2+m7j/n_arms+
    m_joint)*l4)/(density*y_finger*z_finger)));

```

```

88 x_finger2 = (l4+l_j2e)-sqrt((l4+l_j2e)^2-4*(1/2)*-((m2+m7j/n_arms+
      m_joint)*l4)/(density*y_finger*z_finger)));
89
90
91 % x_finger1 = (l_j2e+l4)+sqrt((l_j2e+l4)^2-4*0.5*-((Upp_panto)/(y_finger*
      z_finger)));
92 % x_finger2 = (l_j2e+l4)-sqrt((l_j2e+l4)^2-4*0.5*-((Upp_panto)/(y_finger*
      z_finger)));
93 x_finger = max(x_finger1,x_finger2);
94 %bal = side1-side2
95 check_fing_bal = (x_finger/2-l_j2e-l4)*x_finger*y_finger*z_finger*density
      -(m7j/n_arms+m2+m_joint)*l4;
96 m4 = x_finger*y_finger*z_finger*density;
97 m10 = m4;
98
99 %manuel overwrite other shape finger
100 m4 = 0.053036163187271;%0.055575132029231;%0.058229805666138;
101 m10 = m4;
102 l_com4 = 0.024631157877283;%0.025370942195569;%60.56534182*10^-3-l_j2e-l4
      ;%57.8373162259695*10^-3-l_j2e-l4%57.99699317*10^-3-l_j2e-l4;
103
104 %% Calculations for balanced gripper
105 %CoM specific lengths
106 l_com1 = 95.56*10^-3;
107 l_com2 = l2+(-CoM2_link*m2_link + 2*(l_j2e+btwn_length/2)*btwn_length*
      square_stock_1*square_stock_2*density + (l_j2e+btwn_length+x_counter
      /2)*x_counter*y_counter*z_counter*density)/m2;%l2+(m7j/2*l2)/m2
      ;%141.64*10^-3;
108 l_com3 = (0*(m6j/n_arms)+CoM3_link_j*m3j+(m2+m7j/n_arms+m4+m_joint)*l3)/(
      m2+m_joint+m6j/n_arms+m4+m3j+m7j/n_arms);
109 %l_com4 = x_finger/2-l4-l_j2e;%(l4*(m2+m7j/2+m_joint))/m4;%from CoM of m2
      +m7/2 and m4 which needs to be at the foot of the lower pantograph
110 l_com8 = l_com2;%141.64*10^-3;
111 l_com9 = l_com3;
112 l_com10 = l_com4;
113
114
115 check_m2_bal = (l_com2-l2)*m2-l2*m7j/n_arms;
116
117 %calculate length of small pantograph arm for balance
118 l11 = ((m7j/n_arms+m2+m_joint+m4+m3j+m6j/n_arms)*(m_joint+m5)*l_com3 -
      m5j*CoM5_link*m5)/(2*(m7j/n_arms+m2+m_joint+m4+m3j+m6j/n_arms)*(
      m_joint+m5)+m5j*m_joint);
119 l5 = l11;%+.0271575458043;
120
121 l_com5 = (m5*CoM5_link+m_joint*l5)/(m5+m_joint);
122 l_com11 = l_com5;
123
124
125 %Check pantograph
126 % m1 p1 = m2 a1 + m3 p3
127 % m1 q1 = m3 q3

```

```

128 % m2 p2 = m1 a2 + m4 p4
129 % m2 q2 = m4 q4
130 M1 = m7j/n_arms+m2+m_joint+m4+m3j+m6j/n_arms;
131 M2 = m7j/n_arms+m8+m_joint+m10+m9j+m6j/n_arms;
132 M3 = m11j;
133 M4 = m5j;
134 A1 = l11;
135 A2 = l5;
136 P1 = l_com3;
137 P2 = l_com9;
138 P3 = l_com11;
139 P4 = l_com5;
140
141 Check_panth_l = M1*P1-M2*A2-M3*P3;
142 Check_panth_r = M2*P2-M1*A2-M4*P4;
143
144
145
146 % %m2+m6/2+m4+m3+m7/2
147 %
148 % lCoM3 = (0*(m7/2)+l_com3*m3+(m2+m6/2+m4)*l3)/(m2+m6/2+m4+m3+m7/2);
149 % a1 = (0*(m7/2)+l_com3*m3+(m2+m6/2+m4)*l3)/(m2+m4+m3+m8+m6+m10+m9+m7+m11
      /2);
150
151 m_tot = m1+m2+m3+m4+m5+m6+m7+m8+m9+m10+m11;
152
153 %% Starting positions CoM's of elements
154 l_A1 = 90*10^-3;
155 l_A2 = 110*10^-3;
156
157 % x1 = 0;
158 % y1 = l_com1;
159 % phi1 = 0;
160
161 x3 = -16/2-CoM3_link_j*sin(pi-acos(l_A1/(2*15)));
162 y3 = l_A1 +CoM3_link_j*cos(pi-acos(l_A1/(2*15)));
163 phi3 = pi-acos(l_A1/(2*15));
164
165 li = sqrt(l3^2+(l_A2-l_A1)^2-2*l3*(l_A2-l_A1)*cos(phi3));
166 phi3li = acos(-((l_A2-l_A1)^2 + li^2 + l3^2)/(2*li*l3));
167 phili4 = acos(-((l2^2) + li^2 + l4^2)/(2*li*l4));
168
169 phi4 = phi3-pi + phi3li + phili4;
170 x4 = -16/2-l3*sin(phi3)+l_com4*sin(phi4);
171 y4 = l_A1+l3*cos(phi3)-l_com4*cos(phi4);
172 %balance term
173 phi2 = pi - atan(-((16/2)+x4-(l_com4+l4)*sin(phi4))/(l_A2 - (y4+(l_com4+
      l4)*cos(phi4)))));
174 x2 = -16/2-l_com2*sin(phi2);
175 y2 = l_A2+l_com2*cos(phi2);
176
177 x5 = -16/2 - l_com5*sin(acos(l_A1/(2*15)));

```

```

178 y5 = l_com5*cos(acos(l_A1/(2*15)));
179 phi5 = acos(l_A1/(2*15));
180 x6 = 0;
181 y6 = l_A1;
182 phi6 = 0;
183 x7 = 0;
184 y7 = l_A2;
185 phi7 = 0;
186
187 x9 = 16/2-CoM9_link_j*sin(-pi + acos(l_A1/(2*111)));
188 y9 = l_A1 +CoM9_link_j*cos(-pi+acos(l_A1/(2*111)));
189 phi9 = -pi + acos(l_A1/(2*111));
190
191
192 li2 = sqrt(19^2+(l_A2-l_A1)^2-2*19*(l_A2-l_A1)*cos(phi9));
193 phi9li = acos(-((l_A2-l_A1)^2) + li2^2 + 19^2)/(2*li2*19);
194 phili10 = acos(-(18^2) + li2^2 + 110^2)/(2*li2*110);
195
196 phi10 = phi9+pi - phi9li -phili10;
197 x10 = 16/2-19*sin(phi9)+l_com10*sin(phi10);
198 y10 = l_A1+19*cos(phi9)-l_com10*cos(phi10);
199
200 phi8 = -pi+atan(((16/2)+x10-(110+l_com10)*sin(phi10))/(l_A2 - (y10+(110
+1_com10)*cos(phi10))));
201 x8 = 16/2-l_com8*sin(phi8);
202 y8 = l_A2+l_com8*cos(phi8);
203
204 x11 = 16/2 + l_com5*sin(acos(l_A1/(2*111)));
205 y11 = l_com5*cos(acos(l_A1/(2*111)));
206 phi11 = -acos(l_A1/(2*111));
207
208 %% model parameters
209
210 % linkage positions
211 X = [-17/2, l_A2; %
point1
212 0, l_A2; %point2
213 -16/2, l_A1; %point3
214 0, l_A1; %point4
215 -16/2, 0; %point5
216 -16/2-15*sin(phi5), 15*cos(phi5); %point6
217 -17/2-12*sin(phi2), l_A2+12*cos(phi2); %point7
218 -16/2-13*sin(phi3), l_A1+13*cos(phi3); %point8
219 17/2, l_A2; %point9
220 16/2, l_A1; %point10
221 16/2, 0; %point11
222 16/2-111*sin(phi11), 111*cos(phi11); %point12
223 17/2-18*sin(phi8), l_A2+18*cos(phi8); %point13
224 16/2-19*sin(phi9), l_A1+19*cos(phi9); %point14
225 0, 0]; %point15/origin
226
227

```

```

228 %mass positions
229 %x1 ,y1 ; %m1 point hoeft niet want beweegt niet
230
231 XM = [ x2 ,y2 ; %m2 point
232         x3 ,y3 ; %m3 point
233         x4 ,y4 ; %m4 point
234         x5 ,y5 ; %m5 point
235         x6 ,y6 ; %m6 point
236         x7 ,y7 ; %m7 point
237         x8 ,y8 ; %m8 point
238         x9 ,y9 ; %m9 point
239         x10,y10; %m10 point
240         x11,y11;];%m11 point
241 %%
242 init_build('2D')
243
244
245 bm1_1 = add_plbeam(X(15,:),X(5,:), 1);
246 bm1_2 = add_plbeam(X(15,:),X(11,:), 1,{'transrot_p',bm1_1,'p'});
247 bm5 = add_plbeam(X(5,:),X(6,:), 1,{'trans_p',bm1_1,'q'});
248 bm3_1 = add_plbeam(X(3,:),X(6,:), 1,{'trans_q',bm5,'q'});
249 bm3_2 = add_plbeam(X(6,:),X(8,:), 1,{'transrot_p',bm3_1,'q'});
250 bm6_1 = add_plbeam(X(4,:),X(3,:), 1,{'trans_q',bm3_1,'p'});
251 bm6_2 = add_plbeam(X(4,:),X(10,:), 1,{'transrot_p',bm6_1,'p'});
252 bm11 = add_plbeam(X(11,:),X(12,:), 1,{'trans_p',bm1_2,'q'});
253 bm9_1 = add_plbeam(X(10,:),X(12,:), 1,{'trans_p',bm6_2,'q'},{'trans_q',
    bm11,'q'});
254 bm9_2 = add_plbeam(X(12,:),X(14,:), 1,{'transrot_p',bm9_1,'q'});
255 bm4 = add_plbeam(X(8,:),X(7,:), 1,{'trans_p',bm3_2,'q'});
256 bm10 = add_plbeam(X(14,:),X(13,:), 1,{'trans_p',bm9_2,'q'});
257 bm2 = add_plbeam(X(1,:), X(7,:), 1,{'trans_q',bm4,'q'});
258 bm8 = add_plbeam(X(9,:),X(13,:), 1,{'trans_q',bm10,'q'});
259 bm7 = add_plbeam(X(1,:),X(9,:), 1,{'trans_p',bm2,'p'},{'trans_q',bm8,
    'p'});
260
261
262 bmm3 = add_plbeam(X(6,:),XM(2,:), 1,{'transrot_p',bm3_1,'q'});
263 bmm5 = add_plbeam(X(5,:),XM(4,:), 1,{'transrot_p',bm5,'p'});
264 bmm6 = add_plbeam(X(3,:),XM(5,:), 1,{'transrot_p',bm6_1,'q'});
265 bmm9 = add_plbeam(X(12,:),XM(8,:), 1,{'transrot_p',bm9_1,'q'});
266 bmm11 = add_plbeam(X(11,:),XM(10,:), 1,{'transrot_p',bm11,'p'});
267 bmm4 = add_plbeam(X(8,:),XM(3,:), 1,{'transrot_p',bm4,'p'});
268 bmm10 = add_plbeam(X(14,:),XM(9,:), 1,{'transrot_p',bm10,'p'});
269 bmm2 = add_plbeam(X(7,:),XM(1,:), 1,{'transrot_p',bm2,'q'});
270 bmm8 = add_plbeam(X(13,:),XM(7,:), 1,{'transrot_p',bm8,'q'});
271 bmm7 = add_plbeam(X(1,:),XM(6,:), 1,{'transrot_p',bm7,'p'});
272
273
274 add_nodalloads('xm',XM(2,:), {'trans_p',bmm3,'q'},m3j);
275 add_nodalloads('xm',XM(4,:), {'trans_p',bmm5,'q'},m5j);
276 add_nodalloads('xm',XM(5,:), {'trans_p',bmm6,'q'},m6j);
277 add_nodalloads('xm',XM(8,:), {'trans_p',bmm9,'q'},m9j);

```

```

278 add_nodalloads('xm',XM(10,:),{'trans_p',bmm11,'q'},m11j);
279 add_nodalloads('xm',XM(3,:),{'trans_p',bmm4,'q'},m4);
280 add_nodalloads('xm',X(7,:),{'trans_p',bm4,'q'},m_joint);
281 add_nodalloads('xm',XM(9,:),{'trans_p',bmm10,'q'},m10);
282 add_nodalloads('xm',X(13,:),{'trans_p',bm10,'q'},m_joint);
283 add_nodalloads('xm',XM(1,:),{'trans_p',bmm2,'q'},m2);
284 add_nodalloads('xm',XM(6,:),{'trans_p',bmm7,'q'},m7j);
285 add_nodalloads('xm',XM(7,:),{'trans_p',bmm8,'q'},m8);
286
287
288 add_constrdofs('fix',X(15,:),{'trans',bm1_1,'p'},[1,2]);
289 add_constrdofs('fix',X(15,:),{'rot',bm1_1,'p'},[1]);
290
291
292 add_constrdofs('fix',X(4,:),{'trans',bm6_1,'p'},[1]);
293 add_constrdofs('fix',X(4,:),{'rot',bm6_1,'p'},[1]);
294 add_constrdofs('fix',X(1,:),{'trans',bm7,'p'},[1]);
295 add_constrdofs('fix',X(1,:),{'rot',bm7,'p'},[1]);
296
297     add_inputs('inputx',X(1,:),{'trans',bm7,'p'},[2],[1_A2,-0.07,0]);
298 add_inputs('inputx',X(4,:),{'trans',bm6_1,'p'},[2],[1_A1,-0.07,0]);
299
300
301
302 build_model('Check_combo',{'timestep 1 100'})
303
304 %% run model
305 spacar(-1,'Check_combo');
306 spavisual('Check_combo',1)
307
308 %%
309
310 mass = [m3j m5j m6j m9j m11j m4 m_joint m10 m_joint m2 m7j m8].';
311 nodes = [41 43 45 47 49 51 28 53 31 55 59 57];
312
313 CoMx = (x(:,lnp(nodes,1))*mass)/sum(mass);
314 CoMy = (x(:,lnp(nodes,2))*mass)/sum(mass);
315
316 figure
317 title('Center of mass')
318 subplot(2,1,1)
319 plot(time,CoMx)
320 title('CoMx')
321 subplot(2,1,2)
322 plot(time,CoMy-3.733580507763*10^-3)
323 title('CoMy')
324
325 %%
326 % plot base reaction forces x,y
327 figure
328 plot(time,fxtot(:,lnp(1,1:2)))
329 title('Reaction Forces at Base')

```

```

330 xlabel('time')
331 ylabel('force')
332 legend('fx','fy')
333 % ylim([-1 1]*10^-25)
334
335 figure
336 plot(time,fxtot(:,lnp(1,2)))
337 hold on
338 plot(time,fxtot(:,lnp(15,2)))
339 plot(time,fxtot(:,lnp(33,2)))
340 plot(time,fxtot(:,lnp(15,2))+fxtot(:,lnp(33,2)))
341 title('Reaction Forces at Base v actuator')
342 xlabel('time')
343 ylabel('force')
344 legend('reaction at base','force at lA_1','force at lA_2','total actuator
      ')
345 grid on
346
347 figure
348 plot(time,fxtot(:,lnp(1,2))+fxtot(:,lnp(15,2))+fxtot(:,lnp(33,2)))
349 title('Reaction forces at base minus actuation forces')
350 grid on
351
352 % figure
353 % plot(x(:,lnp(nodes,1)),x(:,lnp(nodes,2)))
354 % legend('2','3','4','5','6','7','8','9','10','11')
355 % title('Motion of the CoM's')

```

APPENDIX J
MATLAB CODE ACTUATED TEST

```
1 clear all
2 close all
3
4 % tb = top balanced
5 % tu = top unbalanced
6 % bb = bottom balanced
7 % bu = bottom unbalanced
8 % n = no load
9
10 %% plots on/of
11
12 norm_pos = 0;
13 raw_amp = 0;
14 all_pos_cycles_separate = 0;
15 std_pos = 0;
16 all_amp_cycles_separate = 0;
17 raw_F = 0;
18 std_amp = 0;
19 std_F = 0;
20 comp_amp = 0;
21 comp_F = 1;
22
23 %% input data from .txt
24 [timetb, postb, input_texttb, input_bintb, Act_stattb, Amp_metertb] =
    readvars('2023-06-25 19-22-13 bal top 20 cpm 40mm 1 sec.txt');
25 [timetu, postu, input_texttu, input_bintu, Act_stattu, Amp_metertu] =
    readvars('2023-06-25 18-12-23 unbal top 20cpm 1 sec trans 40 mm.txt');
26 [timebb, posbb, input_textbb, input_binbb, Act_statbb, Amp_meterbb] =
    readvars('2023-06-17 16-47-41 act low 20 CPM 40 mm 1 sec tran A pos.
    txt');
27 [timebu, posbu, input_textbu, input_binbu, Act_statbu, Amp_meterbu] =
    readvars('2023-06-18 16-04-35 low 20 CPM 40 mm 1sec trans unbal.txt');
28 [timen , posn , input_textn , input_binn , Act_statn , Amp_metern ] =
    readvars('2023-06-25 17-56-19 no load.txt');
29
30
31 gear_circ = 3.6*10^-2; %omtrek metend tandwiel in m
32 encoder_steps = 24; %number of steps of rotary encoder per full turn
33
34 %% raw data and normalised plot
35 if norm_pos == 1
36     figure
37     plot(timetb-timetb(2), (postb-min(postb))/(max(postb)-min(postb)), '
        LineWidth', 2)
38     hold on
39     plot(timetb-timetb(2), input_bintb, 'LineWidth', 2)
40     plot(timetu-timetu(2), (postu-min(postu))/(max(postu)-min(postu)), '
        LineWidth', 2)
```

```

41     plot(timebb-timebb(2), (posbb-min(posbb))/(max(posbb)-min(posbb)), '
        LineWidth', 2)
42     plot(timebu-timebu(2), (posbu-min(posbu))/(max(posbu)-min(posbu)), '
        LineWidth', 2)
43     plot(timen -timen(2) , (posn -min(posn ))/(max(posn )-min(posn )), '
        LineWidth', 2)
44     title('normalised position data')
45     legend('top balanced', 'input', 'top unbalanced', 'bottom balanced', '
        bottom unbalanced', 'no load')
46 end
47
48 amptb = (Amp_metertb-511) * (20/512); % calculating from 10 bit array to
        amps measured 2.5V is 0 Amp 100 mV per step
49 amptu = (Amp_metertu-511) * (20/512); % calculating from 10 bit array to
        amps measured 2.5V is 0 Amp 100 mV per step
50 ampbb = (Amp_meterbb-511) * (20/512); % calculating from 10 bit array to
        amps measured 2.5V is 0 Amp 100 mV per step
51 ampbu = (Amp_meterbu-511) * (20/512); % calculating from 10 bit array to
        amps measured 2.5V is 0 Amp 100 mV per step
52 ampn  = (Amp_metern -511) * (20/512); % calculating from 10 bit array to
        amps measured 2.5V is 0 Amp 100 mV per step
53
54 if raw_amp == 1
55     figure
56     plot(timetb, amptb)
57     hold on
58     plot(timetu, amptu)
59     plot(timebb, ampbb)
60     plot(timebu, ampbu)
61     plot(timen , ampn )
62     title('amparage raw data')
63     legend('top balanced', 'top unbalanced', 'bottom balanced', 'bottom
        unbalanced', 'no load')
64 end
65
66 Ftb = zeros(length(timetb),1);
67 for i=2:length(timetb)
68     if postb(i)-postb(i-1) == 0
69         Ftb(i) = 0;
70     else
71         Ftb(i) = 48*amptb(i)*((timetb(i)-timetb(i-1))/1000)/((postb(i)-
            postb(i-1))*gear_circ/encoder_steps);
72     end
73 end
74
75 Ftu = zeros(length(timetu),1);
76 for i=2:length(timetu)
77     if postu(i)-postu(i-1) == 0
78         Ftu(i) = 0;
79     else
80         Ftu(i) = 48*amptu(i)*((timetu(i)-timetu(i-1))/1000)/((postu(i)-
            postu(i-1))*gear_circ/encoder_steps);

```

```

81     end
82 end
83
84 Fbb = zeros(length(timebb),1);
85 for i=2:length(timebb)
86     if posbb(i)-posbb(i-1) == 0
87         Fbb(i) = 0;
88     else
89         Fbb(i) = 48*ampbb(i)*((timebb(i)-timebb(i-1))/1000)/((posbb(i)-
90             posbb(i-1))*gear_circ/encoder_steps);
91     end
92 end
93 Fbu = zeros(length(timebu),1);
94 for i=2:length(timebu)
95     if posbu(i)-posbu(i-1) == 0
96         Fbu(i) = 0;
97     else
98         Fbu(i) = 48*ampbu(i)*((timebu(i)-timebu(i-1))/1000)/((posbu(i)-
99             posbu(i-1))*gear_circ/encoder_steps);
100 end
101
102 Fn = zeros(length(timen),1);
103 for i=2:length(timen)
104     if posn(i)-posn(i-1) == 0
105         Fn(i) = 0;
106     else
107         Fn(i) = 48*ampn(i)*((timen(i)-timen(i-1))/1000)/((posn(i)-posn(i
108             -1))*gear_circ/encoder_steps);
109 end
110
111 if raw_F == 1
112     figure
113     plot(timetb,Ftb)
114     hold on
115     title('Force')
116     plot(timetu,Ftu)
117     plot(timebb,Fbb)
118     plot(timebu,Fbu)
119     plot(timen,Fn)
120     title('Force raw data')
121     legend('top balanced','top unbalanced','bottom balanced','bottom
122         unbalanced','no load')
123 end
124 %% longer time span averaging
125 %
126 % n = 10;
127 %
128 % F_avg = zeros(length(time),1);

```

```

129 % amp_avg = zeros(length(time),1);
130 %
131 % for i=n:n:length(time)
132 %     if pos(i)-pos(i-1) == 0
133 %         Ftb(i) = 0;
134 %     else
135 %         amp_sum = 0;
136 %         for j = 0:n-1
137 %             amp_sum = amp_sum + amp(i-j);
138 %         end
139 %         amp_avg(i) = amp_sum/n;
140 %         F_avg(i) = 48*amp_avg(i)*((time(i)-time(i-n+1))/1000)/((pos(i)-
        pos(i-1))*gear_circ/encoder_steps);
141 %     end
142 % end
143 %
144 %
145 %
146 % figure
147 % plot(time,F_avg)
148 % title('Force average')
149
150 %% Splice data top balanced
151
152 cyclestb = 0;
153 for i = 2:length(timetb)-2
154     if input_bintb(i)-input_bintb(i-1) == -1
155         cyclestb = cyclestb+1;
156     end
157 end
158
159 j = 0;
160 n = 1;
161 timetb_s = zeros(cyclestb,1);
162 postb_s = [0];
163 amptb_s = [0];
164 inputtb_s = [0];
165 Ftb_s = [0];
166 % Ftb_avg_s = [0];
167 % amptb_avg_s = [0];
168
169 for i = 2:length(timetb)-2
170     if input_bintb(i)-input_bintb(i-1) == -1
171         j = j+1;
172         n = 1;
173     end
174
175     if j == 0
176
177     else
178         timetb_s(j,n) = timetb(i);
179         postb_s(j,n) = postb(i);

```

```

180     amptb_s(j,n)    = amptb(i);
181     inputtb_s(j,n) = input_bintb(i);
182     Ftb_s(j,n)     = Ftb(i);
183 %     Ftb_avg_s(j,n) = Ftb_avg(i);
184 %     amptb_avg_s(j,n) = amptb_avg(i);
185     n = n+1;
186     end
187 end
188
189 %% Splice data top unbalanced
190
191 cyclestu = 0;
192 for i = 2:length(timetu)-2
193     if input_bintu(i)-input_bintu(i-1) == -1
194         cyclestu = cyclestu+1;
195     end
196 end
197
198 j = 0;
199 n = 1;
200 timetu_s = zeros(cyclestu,1);
201 postu_s   = [0];
202 amptu_s   = [0];
203 inputtu_s = [0];
204 Ftu_s     = [0];
205 % Ftu_avg_s = [0];
206 % amptu_avg_s = [0];
207
208 for i = 2:length(timetu)-2
209     if input_bintu(i)-input_bintu(i-1) == -1
210         j = j+1;
211         n = 1;
212     end
213
214     if j == 0
215
216     else
217         timetu_s(j,n) = timetu(i);
218         postu_s(j,n)  = postu(i);
219         amptu_s(j,n)  = amptu(i);
220         inputtu_s(j,n) = input_bintu(i);
221         Ftu_s(j,n)    = Ftu(i);
222 %         Ftu_avg_s(j,n) = Ftu_avg(i);
223 %         amptu_avg_s(j,n) = amptu_avg(i);
224         n = n+1;
225     end
226 end
227
228 %% Splice data bottom balanced
229
230 cyclesbb = 0;
231 for i = 2:length(timebb)-2

```

```

232     if input_binbb(i)-input_binbb(i-1) == -1
233         cyclesbb = cyclesbb+1;
234     end
235 end
236
237 j = 0;
238 n = 1;
239 timebb_s = zeros(cyclestb,1);
240 posbb_s = [0];
241 ampbb_s = [0];
242 inputbb_s = [0];
243 Fbb_s = [0];
244 % Fbb_avg_s = [0];
245 % ampbb_avg_s = [0];
246
247 for i = 2:length(timebb)-2
248     if input_binbb(i)-input_binbb(i-1) == -1
249         j = j+1;
250         n = 1;
251     end
252
253     if j == 0
254
255     else
256         timebb_s(j,n) = timebb(i);
257         posbb_s(j,n) = posbb(i);
258         ampbb_s(j,n) = ampbb(i);
259         inputbb_s(j,n) = input_binbb(i);
260         Fbb_s(j,n) = Fbb(i);
261         % Fbb_avg_s(j,n) = Fbb_avg(i);
262         % ampbb_avg_s(j,n) = ampbb_avg(i);
263         n = n+1;
264     end
265 end
266
267 %% Splice data bottom unbalanced
268
269 cyclesbu = 0;
270 for i = 2:length(timebu)-2
271     if input_binbu(i)-input_binbu(i-1) == -1
272         cyclesbu = cyclesbu+1;
273     end
274 end
275
276 j = 0;
277 n = 1;
278 timebu_s = zeros(cyclesbu,1);
279 posbu_s = [0];
280 ampbu_s = [0];
281 inputbu_s = [0];
282 Fbu_s = [0];
283 % Fbu_avg_s = [0];

```

```

284 % ampbu_avg_s = [0];
285
286 for i = 2:length(timebu)-2
287     if input_binbu(i)-input_binbu(i-1) == -1
288         j = j+1;
289         n = 1;
290     end
291
292     if j == 0
293
294     else
295         timebu_s(j,n) = timebu(i);
296         posbu_s(j,n) = posbu(i);
297         ampbu_s(j,n) = ampbu(i);
298         inputbu_s(j,n) = input_binbu(i);
299         Fbu_s(j,n) = Fbu(i);
300 %         Fbu_avg_s(j,n) = Fbu_avg(i);
301 %         ampbu_avg_s(j,n) = ampbu_avg(i);
302         n = n+1;
303     end
304 end
305
306 %% Splice data no load
307
308 cyclesn = 0;
309 for i = 2:length(timen)-2
310     if input_binn(i)-input_binn(i-1) == -1
311         cyclesn = cyclesn+1;
312     end
313 end
314
315 j = 0;
316 n = 1;
317 timen_s = zeros(cyclesn,1);
318 posn_s = [0];
319 ampn_s = [0];
320 inputn_s = [0];
321 Fn_s = [0];
322 % Fn_avg_s = [0];
323 % ampn_avg_s = [0];
324
325 for i = 2:length(timen)-2
326     if input_binn(i)-input_binn(i-1) == -1
327         j = j+1;
328         n = 1;
329     end
330
331     if j == 0
332
333     else
334         timen_s(j,n) = timen(i);
335         posn_s(j,n) = posn(i);

```

```

336     ampn_s(j,n)   = ampn(i);
337     inputn_s(j,n) = input_binn(i);
338     Fn_s(j,n)    = Fn(i);
339 %     Fn_avg_s(j,n) = Fn_avg(i);
340 %     ampn_avg_s(j,n) = ampn_avg(i);
341     n = n+1;
342     end
343 end
344
345 %% plot sliced data
346 if all_pos_cycles_separate ==1
347     figure
348     hold on
349     for i= 1:cycles-1
350         plot(time_s(i,:)-time_s(i,1), (pos_s(i,:)-min(pos_s(i,:)))/(max(
                pos_s(i,:)-min(pos_s(i,:))))
351     end
352     title('position all cycles')
353 end
354
355 if std_pos ==1
356     figure
357     stdshade(((postb_s-min(postb_s(i,:)))/(max(postb_s(i,:)-min(postb_s(
                i,:))))),.1,'b',timetb_s(1,:)-timetb_s(1,1))
358     hold on
359     % plot(time_s(1,:)-time_s(1,1),input_s(1,:), 'LineWidth', 2, 'Color',
        'k')
360 %     stdshade(((postu_s-min(postu_s(i,:)))/(max(postu_s(i,:)-min(
                postu_s(i,:))))),.1,timetu_s(1,:)-timetu_s(1,1))
361 %     stdshade(((posbb_s-min(posbb_s(i,:)))/(max(posbb_s(i,:)-min(
                posbb_s(i,:))))),.1,timebb_s(1,:)-timebb_s(1,1))
362 %     stdshade(((posbu_s-min(posbu_s(i,:)))/(max(posbu_s(i,:)-min(
                posbu_s(i,:))))),.1,timebu_s(1,:)-timebu_s(1,1))
363 %     stdshade(((posn_s -min(posn_s(i,:)))/(max(posn_s(i,:)-min(posn_s
                (i,:))))),.1,timen_s(1,:)-timen_s(1,1))
364     title('normalised position')
365 %     legend('top balanced','top unbalanced','bottom balanced','bottom
                unbalanced','no load')
366 end
367
368 if all_amp_cycles_separate == 1
369     figure
370     hold on
371     for i= 1:cyclestb-1
372         plot(timetb_s(i,:)-timetb_s(i,1), amptb_s(i,:))
373     end
374     for i= 1:cyclestu-1
375         plot(timetu_s(i,:)-timetu_s(i,1), amptu_s(i,:))
376     end
377     for i= 1:cyclesbb-1
378         plot(timebb_s(i,:)-timebb_s(i,1), ampbb_s(i,:))
379     end

```

```

380     for i= 1:cyclesbu-1
381         plot(timebu_s(i,:)-timebu_s(i,1), ampbu_s(i,:))
382     end
383     for i= 1:cyclesn-1
384         plot(timen_s(i,:)-timen_s(i,1), ampn_s(i,:))
385     end
386     title('amp all cycles')
387     legend('top balanced','top unbalanced','bottom balanced','bottom
           unbalanced','no load')
388 end
389
390 if std_amp ==1
391 %Plot mean and std deviation of cycle
392     figure
393     stdshade(amptb_s,.1,[0         0.4470 0.7410],timetb_s(1,:)-timetb_s
           (1,1),50);
394     hold on
395     stdshade(amptu_s,.1,[0.9290 0.6940 0.1250],timetu_s(1,:)-timetu_s
           (1,1),50);
396     stdshade(ampbb_s,.1,[0.4940 0.1840 0.5560],timebb_s(1,:)-timebb_s
           (1,1),50);
397     stdshade(ampbu_s,.1,[0.4660 0.6740 0.1880],timebu_s(1,:)-timebu_s
           (1,1),50);
398     stdshade(ampn_s, .1,[0.3010 0.7450 0.9330],timen_s(1,:) -timen_s(1,1)
           ,50);
399     title('amp std deviation')
400     legend('top balanced mean','top balanced std','top unbalanced mean','
           top unbalanced std','bottom balanced mean','bottom balanced std','
           bottom unbalanced mean','bottom unbalanced std','no load mean','no
           load std')
401     % ylim([-0.5 2])
402 end
403
404 % P_mech is F*s/t = P_elec = U I
405 % F*s/t = U*I
406 % F = U*I*t/s
407
408 if std_F == 1
409     figure
410     stdshade(Ftb_s,.1,[0         0.4470 0.7410],timetb_s(1,:)-timetb_s(1,1)
           ,50);
411     hold on
412     stdshade(Ftu_s,.1,[0.9290 0.6940 0.1250],timetu_s(1,:)-timetu_s(1,1)
           ,50);
413     stdshade(Fbb_s,.1,[0.4940 0.1840 0.5560],timebb_s(1,:)-timebb_s(1,1)
           ,50);
414     stdshade(Fbu_s,.1,[0.4660 0.6740 0.1880],timebu_s(1,:)-timebu_s(1,1)
           ,50);
415     stdshade(Fn_s ,.1,[0.3010 0.7450 0.9330],timen_s(1,:) -timen_s(1,1)
           ,50);
416     title('force std deviation')

```

```

417     legend('top balanced std','top balanced mean','top unbalanced std','
           top unbalanced mean','bottom balanced std','bottom balanced mean',
           'bottom unbalanced std','bottom unbalanced mean','no load std','no
           load mean')
418 %     ylim([-15 15])
419 end
420
421 % figure
422 % stdshade(F_avg_s,.1,'b',time_s(1,:)-time_s(1,1))
423 % title('Force average std deviation')
424
425 amptu_s_avg = zeros(1,length(amptu_s));
426 amptb_s_avg = zeros(1,length(amptb_s));
427 ampbu_s_avg = zeros(1,length(ampbu_s));
428 ampbb_s_avg = zeros(1,length(ampbb_s));
429 ampn_s_avg  = zeros(1,length(ampn_s));
430
431 for i = 1:length(amptu_s)
432     amptu_s_avg(i) = sum(amptu_s(:,i))/cyclestu;
433     amptb_s_avg(i) = sum(amptb_s(:,i))/cyclestb;
434     ampbu_s_avg(i) = sum(ampbu_s(:,i))/cyclesbu;
435     ampbb_s_avg(i) = sum(ampbb_s(:,i))/cyclesbb;
436     ampn_s_avg(i)  = sum(ampn_s(:,i))/cyclesn;
437 end
438
439 Ftu_s_avg = zeros(1,length(Ftu_s));
440 Ftb_s_avg = zeros(1,length(Ftb_s));
441 Fbu_s_avg = zeros(1,length(Fbu_s));
442 Fbb_s_avg = zeros(1,length(Fbb_s));
443 Fn_s_avg  = zeros(1,length(Fn_s));
444
445 for i = 1:length(Ftu_s)
446     Ftu_s_avg(i) = sum(Ftu_s(:,i))/cyclestu;
447     Ftb_s_avg(i) = sum(Ftb_s(:,i))/cyclestb;
448     Fbu_s_avg(i) = sum(Fbu_s(:,i))/cyclesbu;
449     Fbb_s_avg(i) = sum(Fbb_s(:,i))/cyclesbb;
450     Fn_s_avg(i)  = sum(Fn_s(:,i))/cyclesn;
451 end
452
453 %% plot differences balanced vs unbalanced
454 % figure
455 % title('difference top balanced vs unbalanced avg')
456 % hold on
457 % plot(timetu_s(1,:)-timetu_s(1,1),amptu_s_avg-amptb_s_avg)
458 % legend('unbalanced minus balanced')
459
460 if comp_amp == 1
461     figure
462     title('amperage difference top balanced vs unbalanced')
463     hold on
464     stdshade(1*(amptu_s_avg-amptb_s_avg-0.0),0,[0         0.4470 0.7410],
           timetu_s(1,:)-timetu_s(1,1),50);

```

```

465 legend('unbalanced minus balanced')
466 yline(0)
467
468 % figure
469 % title('difference bottom balanced vs unbalanced')
470 % hold on
471 % plot(timebu_s(1,:)-timetu_s(1,1),amptu_s_avg-amptb_s_avg)
472 % legend('unbalanced minus balanced')
473
474 figure
475 title('amperage difference bottom balanced vs unbalanced')
476 hold on
477 stdshade(1*(ampbu_s_avg - ampbb_s_avg+0.0),0,[0 0.4470 0.7410],
         timebu_s(1,:)-timebu_s(1,1),50);
478 legend('unbalanced minus balanced')
479 yline(0)
480
481 figure
482 title('amperage difference top balanced vs no load')
483 hold on
484 stdshade(1*(amptb_s_avg - ampn_s_avg),0.5,[0 0.4470 0.7410],
         timetb_s(1,:)-timetb_s(1,1),50);
485 legend('amperage unbalanced minus balanced')
486 yline(0)
487
488 figure
489 title('amperage difference bottom balanced vs no load')
490 hold on
491 stdshade(1*(ampbb_s_avg-ampn_s_avg+0.01),0.5,[0 0.4470 0.7410],
         timebb_s(1,:)-timebb_s(1,1),50);
492 legend('unbalanced minus balanced')
493 yline(0)
494
495 figure
496 title('amperage difference top unbalanced vs no load')
497 hold on
498 stdshade(1*(amptu_s_avg-ampn_s_avg-0.022),0.5,[0 0.4470 0.7410],
         timetu_s(1,:)-timetu_s(1,1),50);
499 legend('unbalanced minus balanced')
500 yline(0)
501
502 figure
503 title('amperage difference bottom unbalanced vs no load')
504 hold on
505 stdshade(1*(ampbu_s_avg-ampn_s_avg+0.025),0.5,[0 0.4470 0.7410],
         timebu_s(1,:)-timebu_s(1,1),50);
506 legend('unbalanced minus balanced')
507 yline(0)
508 end
509
510 if comp_F == 1
511     figure

```

```

512     stdshade(Fbu_s_avg-Fn_s_avg, .0, [0         0.4470 0.7410], timebu_s(1, :)-
        timebu_s(1, 1), 50);
513     hold on
514     title('force difference bottom unbalanced vs no load')
515     legend('bottom unbalanced minus no load')
516     yline(0)
517 %     ylim([-15 15])
518
519     figure
520     stdshade(Fbb_s_avg-Fn_s_avg, .0, [0         0.4470 0.7410], timebb_s(1, :)-
        timebb_s(1, 1), 50);
521     hold on
522     title('force difference bottom balanced vs no load')
523     legend('bottom balanced minus no load')
524     yline(0)
525 %     ylim([-15 15])
526
527     figure
528     stdshade(Ftu_s_avg-Fn_s_avg, .0, [0         0.4470 0.7410], timetu_s(1, :)-
        timetu_s(1, 1), 50);
529     hold on
530     title('force difference top unbalanced vs no load')
531     legend('top unbalanced minus no load')
532     yline(0)
533 %     ylim([-15 15])
534
535     figure
536     stdshade(Ftb_s_avg-Fn_s_avg, .0, [0         0.4470 0.7410], timetb_s(1, :)-
        timetb_s(1, 1), 50);
537     hold on
538     title('force difference top balanced vs no load')
539     legend('top balanced minus no load')
540     yline(0)
541 %     ylim([-15 15])
542
543     figure
544     stdshade(Fbu_s_avg-Fbb_s_avg, .0, [0         0.4470 0.7410], timebu_s(1, :)-
        timebu_s(1, 1), 50);
545     hold on
546     title('force difference bottom unbalanced vs bottom balanced')
547     legend('bottom unbalanced minus bottom balanced')
548     yline(0)
549 %     ylim([-15 15])
550
551     figure
552     stdshade(Ftu_s_avg-Ftb_s_avg, .0, [0         0.4470 0.7410], timetu_s(1, :)-
        timetu_s(1, 1), 50);
553     hold on
554     title('force difference top unbalanced vs top balanced')
555     legend('top unbalanced minus top balanced')
556     yline(0)
557 %     ylim([-15 15])

```

```
558 |
559 | end
560 |
561 | % figure
562 | % stdshade(Ftb_s, .7, [0 0.4470 0.7410], timetb_s(1,:) - timetb_s
    | (1,1), 50);
563 | % hold on
564 | % title('force top balanced')
565 | %
566 | % figure
567 | % stdshade(Ftu_s, .7, [0.9290 0.6940 0.1250], timetu_s(1,:) - timetu_s
    | (1,1), 50);
568 | % hold on
569 | % title('force top unbalanced')
570 | %
571 | % figure
572 | % stdshade(Fbb_s, .7, [0.4940 0.1840 0.5560], timebb_s(1,:) - timebb_s
    | (1,1), 50);
573 | % hold on
574 | % title('force bottom balanced')
575 | %
576 | % figure
577 | % stdshade(Fbu_s, .7, [0.4660 0.6740 0.1880], timebu_s(1,:) - timebu_s
    | (1,1), 50);
578 | % hold on
579 | % title('force bottom unbalanced')
580 | %
581 | %
582 | % figure
583 | % stdshade(Fn_s , .7, [0.3010 0.7450 0.9330], timen_s(1,:) - timen_s(1,1)
    | , 50);
584 | % hold on
585 | % title('force no load')
```

APPENDIX K
ARDUINO CODE ACTUATED TEST

```
1 // In this version of the PLC the cycling rate is fixed
2 // The cycling rate is written in cycles per minutes
3
4 //=====SETUP=====
5 //---VARIABLES INITIALIZATION---
6 int    delay_time = 0; //Delay time sets amount of data per cycle by
      delaying next measurement
7 float cycle_time = 0; //Cycle duration in ms calculated depending on the
      cycling rate
8
9 bool input_actuator = 0;
10 float cycling_rate = 0; //Cycling rate
11
12 int encoderPos=0;
13 int encoderStepsPerRevolution= 24;
14
15 bool encoderALast= LOW; //remembers the previous state of the encoder pin
      A
16
17 void setup()
18 {
19 //---PIN SETUP---
20 pinMode(11, OUTPUT); // Set the digital pin D1 as output for the signal,
      this output is vizualised by the L13 led
21 pinMode(A0, INPUT); // Set the analog pin A0 as rotary button output with
      multiplier 1 for calculation
22 pinMode(A1, INPUT); // Set the analog pin A1 as rotary button output with
      multiplier 2 for calculation
23 pinMode(A2, INPUT); // Set the analog pin A2 as rotary button output with
      multiplier 4 for calculation
24 pinMode(A3, INPUT); // Set the analog pin A3 as rotary button output with
      multiplier 8 for calculation
25 pinMode(A5, INPUT); // Set the analog pin A5 as Amperage meter input 2.5
      V = 0 100 mV/A max 20 A
26 pinMode( 3, INPUT); // Set to check if output 11 is correct
27 pinMode( 5, INPUT); // Komp-act status actuator controller output
28
29 //--Encoder setup
30 pinMode(7, INPUT); //Encoder pin A
31 pinMode(6, INPUT); //Encoder pin B
32 digitalWrite(7, HIGH); //Set Encoder pin A to HIGH
33 digitalWrite(6, HIGH); //Set Encoder pin B to HIGH
34
35
36 Serial.begin(115200); // open the serial port at 115200 bps:
37 }
38
39 //=====LOOP CODE=====
40 void loop()
```

```
41 {
42 cycling_rate = 20;
43 cycle_time = (60.0*1000.0)/(2*cycling_rate); //---CACLULATE cycle---
44 delay_time = 1;// ms delay inbetween
45
46
47 //---CYCLE---
48 for(int i=0; i<(cycle_time/delay_time)+1; i++) {
49 boolean encoderA= digitalRead(7);
50
51 if ((encoderALast == HIGH) && (encoderA == LOW)){
52 if (digitalRead(6) == LOW){
53 encoderPos--;
54 }
55 else{
56 encoderPos++;
57 }
58 }
59 Serial.print(millis());
60 Serial.print(,);
61 Serial.print(encoderPos);
62 Serial.print(,);
63 encoderALast= encoderA;
64
65 digitalWrite(11, LOW); // Home
66 Serial.print(Low,);
67 Serial.print(digitalRead(11));
68 Serial.print(,);
69 Serial.print(digitalRead(5));
70 Serial.print(,);
71 Serial.println(analogRead(A5));
72 delay(delay_time);
73 }
74 for(int i=0; i<(cycle_time/delay_time)+1; i++) {
75 bool encoderA= digitalRead(7);
76 if ((encoderALast == HIGH) && (encoderA == LOW)){
77 if (digitalRead(6) == LOW){
78 encoderPos--;
79 }
80 else{
81 encoderPos++;
82 }
83 }
84 Serial.print(millis());
85 Serial.print(,);
86 Serial.print(encoderPos);
87 Serial.print(,);
88 encoderALast= encoderA;
89
90 digitalWrite(11, HIGH); //Extended
91 Serial.print(High,);
92 Serial.print(digitalRead(11));
```

```
93 Serial.print(,);
94 Serial.print(digitalRead(5));
95 Serial.print(,);
96 Serial.println(analogRead(A5));
97 delay(delay_time);
98 }
99 }
```
